



UNIVERSITY OF LEEDS

This is a repository copy of *Self-assembling cashew gum-graft-poly lactide copolymer nanoparticles as a potential amphotericin B delivery matrix.*

White Rose Research Online URL for this paper:
<http://eprints.whiterose.ac.uk/170830/>

Version: Accepted Version

Article:

Richter, AR, Carneiro, MJ, de Sousa, NA et al. (9 more authors) (2020) Self-assembling cashew gum-graft-poly lactide copolymer nanoparticles as a potential amphotericin B delivery matrix. *International Journal of Biological Macromolecules*, 152. pp. 492-502. ISSN 0141-8130

<https://doi.org/10.1016/j.ijbiomac.2020.02.166>

© 2020, Elsevier B.V. This manuscript version is made available under the CC-BY-NC-ND 4.0 license <http://creativecommons.org/licenses/by-nc-nd/4.0/>.

Reuse

This article is distributed under the terms of the Creative Commons Attribution-NonCommercial-NoDerivs (CC BY-NC-ND) licence. This licence only allows you to download this work and share it with others as long as you credit the authors, but you can't change the article in any way or use it commercially. More information and the full terms of the licence here: <https://creativecommons.org/licenses/>

Takedown

If you consider content in White Rose Research Online to be in breach of UK law, please notify us by emailing eprints@whiterose.ac.uk including the URL of the record and the reason for the withdrawal request.



eprints@whiterose.ac.uk
<https://eprints.whiterose.ac.uk/>

1
2 <https://doi.org/10.1016/j.ijbiomac.2020.02.166>

3
4 **SELF-ASSEMBLING CASHEW GUM-GRAFT-POLYLACTIDE COPOLYMER**
5 **NANOPARTICLES AS A POTENTIAL AMPHOTERICIN B DELIVERY**
6 **MATRIX**

7
8 Ana Rosa Richter ^a, Maria J. Carneiro ^a, Nayara A. de Sousa ^b, Vicente P. T. Pinto
9 ^b, Rosimeyre S. Freire, R. ^c, Jeanlex S. de Sousa ^c, Josilayne de Fátima Souza Mendes ^d,
10 Raquel Oliveira dos Santos Fontenelle ^d, Judith P. A. Feitosa ^a, Haroldo C. B. Paula ^a,
11 Francisco M. Goycoolea ^e, Regina C. M. de Paula. ^{a*}

12
13 ^aDepartament of Organic and Inorganic Chemistry – UFC – CEP, Caixa Postal 6021 –
14 Humberto Monte s/n, Campus do Pici, 60455-760 Fortaleza, Brazil.

15
16 ^bFaculty of Medicine – UFC – CEP 62.042-280 – Comandante Mauro Célio Rocha
17 Pontes, 100, Derby, Sobral, Brazil.

18
19 ^cDepartment of Physics – UFC, Fortaleza, Brazil

20
21 ^dCurso de Ciências Biológicas, Centro de Ciências Agrárias e Biológicas, Universidade
22 Estadual do Vale do Acaraú.

23
24 ^eSchool of Food Science and Nutrition, University of Leeds, Leeds LS16 7PA, U.K.

25
26
27 **ABSTRACT**

28
29 Amphotericin B is an antibiotic used in the treatment of fungal disease and leishmania;
30 however, it exhibits side effects to patients, hindering its wider application. Therefore,
31 nanocarriers have been investigated as delivery systems for amphotericin B (AMB) in
32 order to decrease its toxicity, besides increase bioavailability and solubility.
33 Amphiphilic copolymers are interesting materials to encapsulate hydrophobic drugs
34 such as AMB, hence copolymers of cashew gum (CG) and L-lactide (LA) were
35 synthesized using two different CG:LA molar ratios (1:1 and 1:10). Data obtained
36 revealed that copolymer nanoparticles present similar figures for particle sizes and zeta
37 potentials; however, particle size of encapsulated AMB increases if compared to
38 unloaded nanoparticles. The 1:10 nanoparticle sample has better stability although
39 higher polydispersity index (PDI) if compared to 1:1 sample. High amphotericin
40 (AMB) encapsulation efficiencies and low hemolysis were obtained. AMB loaded
41 copolymers show lower aggregation pattern than commercial AMB solution. AMB
42 loaded nanoparticles show antifungal activities against four *C. albicans* strains. It can be
43 inferred that cashew gum/polylactide copolymers have potential as nanocarrier systems
44 for AMB.
45
46
47
48
49
50
51
52
53
54
55
56
57
58
59

60
61
62 Keys words: Poly(lactic acid), cashew gum, nanoparticles, amphotericin B, **antifungal**
63 **activity.**
64

65 Correspondent author: Regina Célia Monteiro de Paula rpaula@dqi.ufc.br
66

67
68 Department of Organic and Inorganic Chemistry – UFC – CEP, Caixa Postal 6021 –
69 Humberto Monte s/n, Campus do Pici, 60455-760 Fortaleza, Brazil
70
71
72
73
74
75
76
77
78
79
80
81
82
83
84
85
86
87
88
89
90
91
92
93
94
95
96
97
98
99
100
101
102
103
104
105
106
107
108
109
110
111
112
113
114
115
116
117
118

119
120
121
122
123 **1. Introduction**
124
125

126 Amphiphilic polymers have been widely investigated as drug delivery system due to
127 their ability to form nanoparticles by self-assembly. The hydrophobic core of
128 amphiphilic nanoparticles can incorporate hydrophobic drugs and delivery them to
129 specific targets [1,2].
130

131
132 Polysaccharides have been used as matrix building blocks to produced amphiphilic
133 materials through the insertion of hydrophobic groups or the grafting of hydrophobic
134 monomers onto polysaccharide chains. The choice of polysaccharide is based on its
135 properties (biodegradability and non-toxicity) and the source material (renewable
136 resource) as well as the presence of several chemical groups, such as hydroxyl, sulfate,
137 amino and carboxyl, which can be used to promote the synthesis.
138
139

140 Lactic acid is obtained by microbial fermentation and source materials include corn
141 syrup, sucrose from sugar cane, lactose cheese pulp and paper [3,4]. Poly (lactic acid)
142 (PLA) is biocompatible, bio-absorbable and biodegradable and it has been approved by
143 the US Food and Drug Administration (FDA) as a biomaterial [5,6]. Copolymers of
144 PLA and polysaccharides, such as cellulose, starch, chitosan and pullulan have been
145 reported [7-16]. Recent studies have addressed synthesis methods and applications as
146 well as the development of potential delivery systems for hydrophobic drugs, due to the
147 capacity to form amphiphilic micelles through self-organization [7-16].
148
149

150 Cashew gum (CG) is an exudate polysaccharide obtained from the *Anacardium*
151 *occidentale* tree, which shows the potential for commercial use due to the large
152 plantations of these trees in Brazil and in other countries [17]. The number of articles
153 published on cashew gum has increase significantly in the past decade. The gum is a
154 branched macromolecule mainly composed of three types of galactan units within the
155 core, linked by C-1 and C-3; C-1 and C-6; and C-1, C-3 and C-6 [18,19]. Copolymers
156 of CG with monomers such as acrylamide [20-24]; acrylic acid [25] and
157 isopropylacrylamide [26] have been reported.
158
159

160 CG gum has also been cited as a potential drug delivery system for epirubicin [26],
161 astaxanthin [27], diclofenac diethyl amine [28], indomethacin [29,30], bovine serum
162 albumin (BSA) [31], pilocarpine [32], isoxsuprine HCl [33], alkaloid epiisopiloturine
163 [34] and insulin [35].
164
165
166
167
168
169
170
171
172
173
174
175
176
177

178
179
180 Richter et al, 2018 [36] reported proof-of-concept of the feasibility to prepare
181 Pickering emulsion systems based on copolymer derivative of cashew gum and L-
182 poly lactide. The systems offered the possibility to associate AMB with encapsulation
183 efficiencies up to 47 %, however the synthesis and characterization of copolymer
184 neither the production and characterization of nanoparticles by self-assembling were
185 reported.

186
187
188
189
190 Amphotericin B (AMB) was the drug selected to be loaded into the self-assembled
191 nanoparticles. AMB is a potent fungistatic and fungicide drug produced by the
192 actinomycetes *Streptomyces nodosus* [37] that was approved for clinical use by FDA
193 in 1959 [38]. AMB is also prescribed in the treatment of visceral leishmaniasis. It is a
194 lipophilic drug that binds to lipids and intercalates into lipid bilayers that then associate
195 to form transmembrane pores [39]. AMB also shows very low oral bioavailability due
196 to its structural features that violate Lipinsky's rule (e.g., low Log P, high Mw, large
197 polar surface area). Hence, novel pharmaceutical formulations of AMB are of great
198 interest with a view to contribute to increase its pharmacological bioavailability for oral
199 and other routes of administration, while exerting control on its drug release.

200
201
202
203
204
205
206
207
208
209
210
211
212
213
214
215
216
217
218
219
220
221
222
223
224
225
226
227
228
229
230
231
232
233
234
235
236

Many authors have proposed new encapsulation techniques for AMB in order to decrease its side effects and toxicity, such as: nanoparticles [40-43], micelles [44,45], conjugates [46] and emulsions [36,47,48].

In this study, cashew gum/poly lactide copolymers (CGPLAP) with different CG:PLA molar ratios have been synthesized and characterized by resonance magnetic nuclear (RMN) and infrared spectroscopy. The effect of copolymer composition on physicochemical characteristics of AMB loaded and unloaded nanoparticles obtained by self-assembling were evaluated and compared with Pickering emulsion system previously reported [36].

2. Experimental

2.1. Materials

Cashew tree (*Anacardium occidentale*) exudate was kindly donated by EMBRAPA (Empresa Brasileira de Pesquisa Agropecuária) and the cashew gum (CG) was isolated as described in a previously paper [18]. L-Lactide (3,6-dimethyl-1,4-dioxane-2,5-dione), triethylamine (TEA) and Amphotericin B solution were purchased from Sigma-Aldrich

237
238
239 and used without further purification. The cashew gum used in this study has an average
240 molar mass, obtained by size exclusion chromatography, of $6.9 \times 10^4 \text{ g}\cdot\text{mol}^{-1}$ and the
241 molar sugar ratio for galactose:glucose:arabinose:rhamnose:glucuronic acid was
242 determined as 1.00:0.20:0.08:0.05:0.06.
243
244
245
246

247 2.2. *Cashew gum/lactide copolymer (CGPLAP)*

248

249
250 The copolymers were synthesized as previously reported by Seo et al. [13]. Briefly,
251 1.0 g of CG was dissolved in DMSO in the temperature range of 70-75°C, under
252 magnetic stirring. L-Lactide and TEA were added to the flask (the amounts of reagents
253 and solvent are given in Table 1) and the reaction was kept under N_2 atmosphere for 2 h.
254 After this time, the N_2 flow was interrupted and the reaction was left to proceed for 10
255 h. At the end of the reaction time, the copolymer solution was filtered, dialyzed against
256 water and lyophilized. The graft reaction was performed in two CG:PLA molar ratios
257 (1:1 and 1:10). In this methodology, the concentration of lactide and TEA was kept at
258 10 and 2% (w/v), respectively. To remove residual monomer and/or homopolymer
259 formed during the reaction, hexane was added to the lyophilized graft copolymers
260 dispersed in distilled water and the system was kept under magnetic stirring for 48 h
261 [49]. After this period of time, the aqueous phase was removed and lyophilized. The
262 purified samples were named CGPLAP.
263
264
265
266
267
268
269
270
271
272
273

274 2.3. *Characterization of cashew gum copolymer*

275

276
277 The Fourier transform IR (FT-IR) spectra were recorded on an FTLA 2000, ABB
278 Bomem spectrometer, in the range of 400 - 4000 cm^{-1} , with the samples as KBr pellet.
279 ^1H NMR spectra were recorded in DMSO-d_6 at 353 K on a Fourier transform Bruker
280 Advance DRX 500 spectrometer with an inverse multinuclear gradient probehead
281 equipped with z-shielded gradient coils and a Silicon Graphics workstation. The molar
282 substitution (MS), degree of substitution (DS) and degree of polymerization (DP) were
283 calculated based on procedures reported in the literature by Guo et al. [5] and Teramoto
284 and Nishio [50] with modifications:
285
286
287
288
289
290
291
292
293
294
295

296
297
298
299 MS = $\frac{(A + B)/3}{H - 1}$
300
301 (1)

302
303
304 DS = $\frac{A/3}{H - 1}$ (2)
305
306

307
308 DP = $\frac{MS}{DS}$ (3)
309
310

311 where A and B are the area of terminal and internal methyl groups, respectively, and H-
312 1 is the area of anomeric protons (5.04 to 5.17 ppm).
313
314

315 316 2.4. *Self-assembled nanoparticles* 317 318

319 Self-assembled nanoparticles were prepared by the dialysis method. GCPLAP (10
320 mg) was dissolved in 10 mL of dimethyl sulfoxide (DMSO) and the solution was
321 dialyzed against distilled water using a dialysis membrane (cut off 14,000 g.mol⁻¹) for 3
322 days. The resulting nanoparticles were stored in a freezer until characterization.
323
324
325
326

327 2.5. *Particle size* 328 329

330 The size and zeta potential nanoparticles were characterized by dynamic light
331 scattering with non-invasive back scattering (DLS-NIBS), at 25°C, with irradiation of
332 the sample using a 4 mW helium/neon red laser ($\lambda=633$ nm). The detection was carried
333 out at an angle of 173°. The zeta potential was measured by mixed laser Doppler
334 velocimetry and phase analysis light scattering (M3-PALS). A Nanosizer ZS 3600
335 system (Malvern Instruments Ltd., Worcestershire, UK) was used for both
336 determinations.
337
338
339
340
341
342

343 2.6 *Stability Study* 344 345

346 The stability experiment was performed with blank nanoparticles. The stability was
347 carried out in phosphate buffer solution (pH 7.4) at 37 °C. The buffer (950 μ L) was
348 added to the nanoparticle solution (50 μ L), and the system was left in an incubator at 37
349
350
351
352
353
354

355
356
357 °C with stirring at 50 rpm. After 20 min, the particle size was measured and this analysis
358 was repeated every 20 min until 360 min. Measurements were made in triplicates.
360
361

362 2.7. Morphology

363
364
365 The morphology of CGPLAP nanoparticles was examined using scanning electron
366 microscopy (SEM) and atomic force microscopy (AFM). CGPLAP nanoparticles were
367 examined using scanning electron microscopy (Quanta FEG 450 - FEI) at a voltage of
368 20 kV. The nanoparticles solutions were fixed in stubs with carbon tape and metallized
369 with gold (Quorum QT150ES).
370
371

372
373 Blank NP's were analyzed using Asylum MFP3D-Bio microscopy (AFM). The
374 images were taken in tapping mode, using an EconoLTESP with nominal spring
375 constant of 5n/m and resonance frequency of 138 Khz. Images acquired in intermittent
376 contact mode (tapping mode). 10 µL of diluted samples (1:200 v/v) was spread onto
377 freshly cleaned mica and vacuum dried.
378
379
380

381 2.8. AmphotericinB encapsulation and aggregation state

382
383
384 An amount of 50 mg of the copolymer and 5 mg of AMB were solubilized in 5 mL of
385 DMSO. The solution with the drug was dialyzed for 72 h against distilled water in a
386 light-protected vessel. For a determination of encapsulation efficiency (EE%), NP's were
387 frozen and lyophilized. The material in powder form was resuspended in DMSO and
388 centrifuged at 40,000 G for 0.5 h so that the matrix of the nanoparticle ruptured and
389 released the encapsulated drug. After centrifugation the AMB concentration was
390 determined by spectrophotometry in visible ultraviolet (UV-vis) without wavelength of
391 391 nm, using a Shimadzu® UV-1800 spectrophotometer.
392
393

394 The amount of AMB encapsulated was calculated using a calibration curve to
395 determine the ratio of absorbance to concentration ($R^2 = 0.9988$). The following
396 formula was used to calculate EE%:
397
398

$$399 \text{EE\%} = \frac{\text{AMB mass in NP}}{\text{initial AMB add to NP}} \times 100\%$$

400
401
402
403
404
405
406
407
408
409
410
411
412
413

414
415
416 To determinate the state of aggregation of AMB in nanoparticles before extraction,
417 the AMB loaded nanoparticles were diluted in deionized water and the UV/vis spectrum
418 registered. The experiment was also performed with a commercial Sigma AMB solution
419 (with sodium desoxycholate).
420
421
422

423 424 *2.9 Hemolysis assay*

425
426 To evaluate the toxicity of self-assembling nanoparticles, its hemolytic activity was
427 tested using human red bloods cells (RBCs). Human bloods was collected in EDTA
428 tubes, washed three times and re-suspended with sterile saline solution (0.9 %). The
429 samples were tested at different AMB concentration from 62.5 to 250 $\mu\text{g.mL}^{-1}$. Triton X
430 and saline solution were used as positive and negative hemolysis control, respectively.
431 The mixture was incubated for 30 min at 37 °C and centrifuged at 8,000 rpm for 1 min.
432 After centrifugation time, the absorbance of samples supernatant was measured at 492
433 nm. The results were statistically compared by Tukey test ($p < 0.05$), using Statistical
434 10.0 program.
435
436
437
438
439
440
441
442

443 444 *2.10 In vitro drug release*

445
446 The release profiles of the drug loaded nanoparticles were obtained using a dialysis
447 system. Each nanoparticle sample (20 mg) were introduced into cellulose acetate
448 membranes (cut off 14,000 g.mol^{-1}) and dialyzed against 30 mL of PBS buffer solution
449 containing 0.25% sodium lauryl sulfate, at pH 7.4, and 37 °C. Aliquots were taken at
450 certain time intervals and analyzed by spectrophotometry in the UV–vis region.
451
452
453
454
455

456 457 *2.11 In vitro antifungal activity*

458
459
460 The minimum inhibitory concentrations (MIC) for blank and AMB-loaded nanoparticle
461 and the Sigma-Aldrich AMB solution were determined via the broth micro dilution
462 method using 96-well plates according to document M27-A3, from the Clinical and
463 Laboratory Standards Institute-CLSI (formerly NCCLS) [51]. Stock solution of
464 nanoparticles ($64 \mu\text{g.mL}^{-1}$) in sodium lauryl sulfate (0.150 mL) were serially diluted to
465
466
467
468
469
470
471
472

473
474
475 range 0.007 – 16 $\mu\text{g}\cdot\text{mL}^{-1}$ in RPMI 1640 medium. AMB (0.007 - 16 $\mu\text{g}\cdot\text{mL}^{-1}$) was used
476
477 as a standard. The microplates were incubated at 35°C and fungal growth/inhibition was
478
479 observed after 48 h. The MIC was defined as the lowest concentration of an
480
481 antimicrobial agent that prevents visible growth of a microorganism. The results were
482
483 read visually as recommended by CLSI [51]. Each experiment was performed in
484
485 duplicate. Four *Candida albicans* strains were used in the experiment, one obtained
486
487 from the American Type Culture Collection (ATCC 90028) and three from clinical
488
489 isolates of *C. albicans* obtained from Santa Casa de Misericórdia Hospital, Sobral
490
491 (Ceará, Brazil).
492
493
494
495
496
497
498

499 **3. Results and discussion**

500
501
502 The grafting of L-lactide onto CG chains involves a nucleophilic attack by the
503
504 hydroxyl groups of the polysaccharide. Since the hydroxyl groups are not sufficiently
505
506 nucleophilic to initiate the reaction, the production of a reactive alkoxide is required.
507
508 This was carried out through the addition of triethylamine (TEA), as suggested by Cho
509
510 et al. [13]. TEA also acts as a catalyst for the lactide ring-opening reaction.

511 *3.1. Cashew gum graft reaction yield*

512
513
514 The reaction yield was higher for CGPLA 1:1 than for CGPLA 1:10 (Table 2),
515
516 indicating that an increase in the amount of L-lactide in the reaction medium leads to a
517
518 decrease in the yield. The CGPLA was purified in order to remove the homopolymer
519
520 produced in a side reaction. Purification of the copolymer was carried out by polylactide
521
522 extraction with a non solvent. Several authors have reported the use of organic solvents,
523
524 such as chloroform [15], toluene [7,52,53], acetone [54] and hexane [49,55], to remove
525
526 the polylactide, or a solvent mixture like toluene/methanol [56]. In this study, hexane
527
528 was chosen to remove the homopolymer. CGPLA copolymers are not soluble in this
529
530 solvent but polylactide is soluble. The yield of the purified copolymer, in relation to the
531

532
533
534 unpurified copolymer, also decreased with increasing of CG:PLA molar ratio. An
535
536 increase in the proportion of lactide in the reaction favored the formation of the
537
538 homopolymer. The percentage (%) of grafting observed for the chitosan-g-poly(lactic
539
540 acid) derivative at a chitosan:PLA ratio of 10:1 was higher (92.49%) than that observed
541
542 for CGPLA in the same feed ratio [10]. Cellulose graft with PLA copolymers, with a
543
544 feed ratio of 1:1, show an increase in the grafting from 27.88 to 32.63 % on varying the
545
546 reaction temperature from 130 to 110°C [5]. These values were also higher than that
547
548 obtained with a CG:PLA ratio of 1:1. In both cited articles, stannous octoate was used
549
550 as the catalyst and high temperatures were employed (110-140 °C). In the CGPLA
551
552 synthesis triethylamine (TEA) was used as a catalyst with the temperature ranging from
553
554 70-75°C.

555 3.2. FTIR analysis

556
557
558 FTIR spectra for the PLA, CG and copolymers are shown in Fig. S1-Supplementary
559
560 material. The PLA spectrum shows intense bands in the range from 2971 to 2853 cm⁻¹
561
562 and at 1739 cm⁻¹. The bands at 2971 and 2853 cm⁻¹ are due to the asymmetric and
563
564 symmetric stretching vibration of CH₃, while the band at 2853 cm⁻¹ is related to the
565
566 symmetric vibration of aliphatic CH groups. The intense band at 1739 cm⁻¹ is attributed
567
568 to the C=O stretching vibration of aliphatic ester groups [56]. The cashew gum
569
570 spectrum (in salt form) shows a broad band at 3379 cm⁻¹ due to O–H stretching
571
572 vibrations. Strong bands at 1150, 1080 and 1030 cm⁻¹ are due to stretching vibrations of
573
574 C–O–C from glycosidic bonds and the bending of O–H from alcohols, characteristic of
575
576 polysaccharide structures. A weak band at 2937 cm⁻¹ was attributed to C–H stretching
577
578 vibrations. The absorption at 1647 cm⁻¹ is due to the O–H scissor vibrations of bonded
579
580 water molecules and the shoulders at ~1600 and 1414 cm⁻¹ can be attributed to
581
582 asymmetrical and symmetrical –COO⁻ vibrations of the uronic acid present in the gum
583
584 [57-59].

585
586 In the copolymers, the presence of a new band at 1739 cm⁻¹, as well as other bands
587
588 characteristic of CG polysaccharide (e.g., 3379, 1150, 1080, 1030 cm⁻¹) confirms the
589
590 insertion of PLA in the CG chains.

591 3.3. NMR spectroscopy

591
592
593
594
595 The NMR spectrum for cashew gum without modification shows characteristic
596 anomeric protons in the region of 4.4 to 5.0 ppm using D₂O as a solvent [73]. The
597 signals in this region are reported to be due to α -D-glucose (4.95 ppm), α -L-rhamnose
598 (4.81 ppm), β -D-galactose (1 \rightarrow 3) (4.69 ppm and 4.43 ppm) and β -D-glucuronic acid
600 (4.51 ppm). The H-2 to H-5 signals are overlapped in the regions of 3.4 ppm to 4.3 ppm
601 and a quartet signal in the region of 1.26 ppm is due to the methyl protons of rhamnose
602 [60].
603

604
605
606 Several polysaccharide/PLA graft copolymers have been investigated using ¹H-NMR
607 spectroscopy. The insertion of PLA leads to signals characteristic of terminal and
608 internal backbone methyl groups at 1.3 ppm (A structure in Fig. 1) and 1.4 ppm (B
609 structure in Fig. 1), respectively. The signals at 5.2 ppm (C structure in Fig. 1) and 4.2
610 ppm (D structure in Fig. 1) were attributed to internal and terminal methine protons of
611 PLA, respectively [7,9,11,61].
612
613

614
615 Fig.1 also shows the ¹H- NMR spectra for the CGPLAP copolymers in DMSO-d₆.
616 Signals due to the lactide insertion into the cashew gum structure, at 1.31, 1.44, 4.2 and
617 5.4 ppm, and signals associated with the anomeric protons of cashew gum in DMSO-d₆
618 (in the region of 5.04 to 5.17 ppm) were observed. The signal associated with the
619 terminal methyl groups at 1.31 ppm is overlapped with that of the methyl groups of
620 rhamnose present in the CG. The presence of the PLA signals related to internal and
621 terminal groups indicates that the PLA chain is grafted onto the CG structure [11] and
622 the absence of a signal at 1.66 ppm, characteristic of the lactide monomer [12], suggests
623 the absence of residual monomer in the purified copolymers.
624
625

626
627
628 The values for MS, DS and DP, based on equations 1 to 3, are reported in Table 2.
629 These values show that the increase in lactide content does not increase the percentage
630 of grafting, since only a small difference can be observed in these values. However, a
631 slight increase in the DP was observed for a CGPLAP ratio of 1:10. The variation in the
632 DP values may lead to different nanoparticle aggregation pattern. This result differs
633 from that obtained for the pullulan graft PLA [12,13], where an increase in the
634 PLA:glycosidic repeating unit ratio from 5:1 to 20:1 led to an increase in the DS (from
635 0.45 to 0.65). However, the DS values obtained for the CGPLAP copolymers are higher
636 than those reported for pullulan:PLA copolymers [12,13].
637
638
639
640
641
642
643
644
645
646
647
648
649

3.4. Particle size

The nanoparticles were prepared via self-organization using DMSO as the solvent. The hydrodynamic diameter, in an aqueous medium, was determined by DLS at 25 °C. Nanoparticle (NP) size distributions for both copolymers are monomodal (see Fig. S2-Supplementary material). The Z-average diameters in distilled water for NP obtained with CGPLAP molar ratios of 1:1 and 1:10 were 230.4 ± 7.7 and 243.6 ± 10.7 nm, respectively. The PDI values were 0.272 ± 0.002 and 0.307 ± 0.018 , respectively for NPs obtained with ratios of 1:1 and 1:10, indicating a narrow size distribution. The CGPLAP 1:10 NPs had a higher PDI value than the CGPLAP 1:1 NPs. An increase in the feed ratio does not affect significantly the hydrodynamic size of the self-assembled CGPLAP nanoparticles. The zeta potentials for the two copolymers were also similar (-26.1 ± 1.9 and -24.3 ± 2.3 mV, respectively, for the CGPLAP copolymers 1:1 and 1:10).

In our previously work [36] we produced Pickering emulsion with monomodal distribution with CGPLAP 1:1 sample using Miglyol as oil phase. The particle size value of this Pickering emulsion was closer to that obtained by self-assembling (241 ± 5 nm). Graft copolymer of PLA with other polysaccharide such chitosan [18], pullulan [11,12], and chondroitin sulfate [61] have been synthesized and characterized by DLS. Chitosan-g-PLA nanoparticles were produced by dialysis and dialysis plus ultrasonification [16]. Dialysis methods led to a particle size of 569 nm, however, when these particles were submitted to ultra sonification with different amplitude and time, particles size ranging from 200 to 350 nm were obtained. For pullulan-g-PLA copolymers nanoparticles prepared with similar methods used in the present work, the particle size decrease with the increase of degree of substitution (DS) ranging from 341 to 202 nm depending on DS [11]. Chondroitin sulfate-g-PLA copolymers nanoparticle were prepared by emulsification (O/W emulsion) with particle size ranging from 92.1 to 108.5 nm, when the of proportion chondroitin sulfate increase in the copolymer the particle size decrease [62].

The stability of the nanoparticles in physiological buffer (pH 7.4 at 37 °C) over 6 h was determined by measuring the particle size (Fig.2) to observe whether aggregation occurred during this period. It can be observed that the copolymers nanoparticles in buffer pH 7.4 (231.4 ± 17.3 and 226.5 ± 18.2 nm for CGPLAP 1:1 and 1:10), respectively have similar size to that observed in distilled water.

709
710
711 The particle size remained almost constant for up to 240 min for both copolymers
712 (Fig. 2a), and the CGPLAP 1:1 NPs are slightly larger compared with the CGPLAP
713 1:10 NPs. After this time, the CGPLAP 1:1 NPs started to aggregate, as observed by the
714 increase in the particle size, however, size distribution is still monodisperse (Figs 2b and
715 2c). The higher stability of the CGPLAP 1:10 NPs may be related to the DP or different
716 substitution patterns at the CG chain.
717
718
719
720

721 722 3.5. Nanoparticles Morphology 723

724
725 SEM and AFM micrographs show that the nanoparticles have spherical shape with a
726 smooth surface (Fig. 3a, 3b, 3c and 3d) and the average nanoparticle sizes are
727 significantly smaller than that obtained by DLS, approximately 70 nm for both
728 CGPLAP 1:1 and CGPLAP 1:10 (Fig 3e and 3f). These differences may be due to the
729 fact that AFM and SEM determine the diameter of the dry particles, and will probably
730 cause them to shrink, whereas the DLS determines the hydrodynamic diameter in
731 aqueous solution, which leads to swelling of the samples and consequently larger
732 particles sizes.
733
734
735
736
737

738 Amplitude and phase images were show in Fig 4. The CGPLAP 1:1 samples are
739 extremely homogeneous, showing no phase difference (Fig 4a and 4c), whereas
740 CGPLAP 1:10 NP's have texture in phase (Fig 4b and 4d). This can be explained by the
741 slight increase in DP, observed for CGPLAP 1:10, that increase PLA chain. The
742 variation on the hydrophobicity may lead to phase difference on the AFM images of
743 CGPLAP 1:10.
744
745
746
747

748 749 3.6. Amphotericin B (AMB) encapsulation and loading efficiency (LE) 750

751
752 The other important aspect to evaluate for the CGPLAP nanoparticles was their
753 capacity to associate AMB, a drug of low water solubility. The use of nanocapsules is
754 reported for protection of different systems in pharmaceutical or cosmetic applications,
755 especially for substances that degrade at temperatures above 40 °C or are sensitive to
756 oxidation in the presence of water, pH variation or ultraviolet light[63]. The loading
757 efficiency were 89.7 and 82.7 (%) for CGPLAP 1:1 and 1:10, respectively. It can be
758 seen that the efficiency value was slightly lower for the GCPLAP 1:10 systems.
759 Pickering emulsions produced with the same copolymers in previous work have a much
760
761
762
763
764
765
766
767

768
769
770 lower encapsulation efficiency (21 to 47 % respectively for Pickering emulsion
771 stabilized with CGPLAP 1:1 and 1:10) compared with self-assembling nanoparticles
772 [36].
773
774

775 Other authors also reported high values for encapsulation efficiency, confirming that
776 amphiphilic systems are efficient in incorporating amphotericin B. Polycarbonate
777 micelles obtained LE values (%) ranging from 66.4 to 76.4 % [44]. AMB-containing
778 PLA-PEG nanoparticles were successfully obtained by the emulsion-solvent
780 evaporation method. The mean diameter in the NPs was 223 ± 25 nm and the
781 encapsulation efficiency were 68.9% [64]. Micelles of linolenic acid-modified PEG-
782 oligochitosan conjugates prepared by dialysis method has 82.27 ± 1.96 % of drug
783 encapsulation efficiency [65]. Nanoparticles of PLGA has efficiency loading
784 approximately 80 % [66]. So our samples were very efficiently in the encapsulation of
785 AMB in comparison with other systems.
786
787
788
789

791 AMB tends to aggregate in commercial formulations, leading to an increase of toxicity.
792 The UV spectroscopy was used to determinate the aggregation states of AMB when
793 encapsulated in nanoparticles. The UV-vis for AMB in DMSO and a commercial
794 solution of AMB from Sigma Aldrich (2×10^{-5} mol.L⁻¹) in water are show in Fig. 5a.
795 Bands located at 407-419 nm (Band IV) is the characteristic peak for monomeric form
796 of AMB, while Band I, at approximately 330-340 nm, represents the aggregated form
797 [45]. The spectrum for AMB in DMSO showed high intensity peaks at 370, 391 and
798 415 nm, representing the monomeric form and a low intensity peak at 353 nm. In
799 contrast, the absorbance spectrum for the commercial AMB solution in water showed a
800 high intensity peak at 327 nm, which represent the aggregate state of AMB and peaks of
801 low intensity at 362, 385 and 408 nm.
802
803
804
805
806
807

808 The UV-vis for the CGPLAP nanoparticles can be seen in Fig 5 band showed a broad
809 peak of high intensity at 332 nm for both copolymers (GCPLAP 1:1 and 1:10). Lower
810 intense peaks were observed at 362, 388 and 419 nm. Spectra with similar absorption
811 profiles were found in polycarbonate micelles [44], cluster dextrin [67], linolenic acid-
812 modified and oligochitosan conjugates micelles [65] and PLGA nanoparticles [66].
813
814

815 In general, the spectral changes induced by the aggregation of AMB may be
816 represented as the value of the ratio of the intensities of the major absorption bands at λ
817 = 348 and 409 nm (i.e., $\sim A_{348}/\sim A_{409}$ ratio). This ratio assumes a value ≥ 2.0 for AMB
818 aggregated species, and of ~ 0.25 for the monomeric form [68].
819
820
821
822
823
824
825
826

827
828
829 In commercial formulations of AMB (e.g., Amphocil®, Fungizone®, Abelcet® and
830 AMBisone®) A_{348}/A_{409} ratios were reported as 9.1, 4.8, 1.3 and 2.9, respectively [69]
831 thus reflecting that AMB occurs in the aggregated form in such all cases, been
832 Abelcet® and AMBisone® in less aggregated form. The A_{332}/A_{419} ratio values for the
833 CGPLAP 1:1 (A_{332}/A_{419} ratio 3.18) and 1:10 (A_{332}/A_{419} ratio 3.28) nanoparticles indicate
834 that the AMB loaded in CGPLAP nanoparticles are in aggregate form, however they are
835 in a less aggregated state than the observed for Amphocil®, Fungizone® [69]. If
836 compared with commercial AMB solution from Sigma-Aldrich (A_{332}/A_{419} ratio 6.12)
837 values obtained for the CGPLAP copolymers are almost half of the value.
838

839 CGPLAP Pickering emulsion was more effective in loaded AMB without
840 aggregation than the nanoparticles produced by self-assembling [36]. The values of
841 A_{348}/A_{409} was 1.7 and 1.6 respectively for CGPLAP 1:1 and 1:10 copolymers Pickering
842 emulsion [36].
843

844 The size, PDI and zeta potential for the CGPLAP nanoparticles unload and load with
845 AMB and for commercial AMB solution (Sigma-Aldrich) is shown in Fig 6. It was
846 possible to observe an expressive increase in the particle size with AMB encapsulation
847 for both systems, with values of 230.4 ± 7.7 and 243.6 ± 10.7 nm for unloaded and 1192
848 ± 23.6 and 1025 ± 143 nm for loaded AMB respectively for CGPLAP 1:1 and 1:10
849 nanoparticle. This occurs, probably due to electrostatic interferences of the drug with
850 the polymer chain during the formation of the nanoparticles [14]. The commercial AMB
851 solution appeared almost four times larger than the two nanoparticle systems, with a
852 value of 3682 ± 231 nm.
853

854 When evaluating the PDI for the nanoparticles, there is a decrease in their values for
855 both, from 0.277 to 0.096 for the nanoparticle CGPLAP 1: 1 and from 0.307 to 0.254
856 for the nanoparticle CGPLAP 1:10. This indicates that the AMB load into the
857 nanoparticles causes the particle size to become more homogeneous. The commercial
858 AMB solution has a higher PDI value (0.413 ± 0.06) than the CGPLAP nanoparticles.
859

860 The zeta potential is another important parameter because indicates the stability of
861 nanoparticles and provides the aggregation. For unload CGPLAP 1:1 and 1:10
862 nanoparticles, has a zeta potential of -26.1 ± 1.9 and -24.3 ± 2.3 mV, respectively. For
863 the load AMB nanoparticles has a decrease in zeta potential value of -10.3 ± 0.2 and
864 -12.7 ± 0.9 mV for GCPLAP 1:1 and 1:10, respectively. The zeta potential for
865

886
887
888 commercial AMB is close to that of nanoparticles without AMB, with a value of $-22.4 \pm$
889
890 0.9 mV.
891

892 893 *3.7 Biocompatibility assessment* 894

895
896 The extent of hemolysis caused after incubation with RBCs is show in Fig 7 for
897 CGPLAP 1:1, CGPLAP 1:10 blank and AMB loaded nanoparticles and commercial
898 AMB. Incubation of RBCs with triton X (0.1%), as a positive control, led to lysis in red
899 cells instantly, causing 100% hemolysis and releasing hemoglobin, which causes the
900 solution to become cloudy after centrifugation, saline solution (0.9%) was used as
901 negative control. Commercial AMB solution shows a large extent of erythrocyte
902 damage.
903
904

905
906 It can be observed for blank nanoparticles (in this case concentration is the
907 copolymer concentration), in the all concentrations studied, there is no statistical
908 difference between CGPLAP 1:1 and CGPLAP 1:10 nanoparticles, with hemolysis
909 extended less than 5%, indicating excellent biocompatibility for nanoparticles matrix.
910
911

912
913 For AMB loaded copolymers the concentration in Fig. 7 refers to AMB
914 concentration. Statistical analysis using Tukey test revealed that the differences between
915 CGPLAP 1:1 + AMB and CGPLAP 1:10 + AMB nanoparticles were significant ($P <$
916 0.05) when the AMB concentrations were 250 and $125 \mu\text{g.mL}^{-1}$.
917
918

919
920 CGPLAP 1:1 + AMB has a lower percentage of hemolysis (47.0 ± 3.7 and 2.7 ± 1.4
921 % respectively for 250 and $125 \mu\text{g.mL}^{-1}$ AMB concentrations) than CGPLAP 1:10 +
922 AMB (85.9 ± 4.2 and 20.5 ± 5.3 % respectively for 250 and $125 \mu\text{g.mL}^{-1}$ AMB
923 concentrations). Despite the high hemolysis for CGPLAP 1:10 + AMB (85.9 ± 4.2 % at
924 AMB concentration of $250 \mu\text{g.mL}^{-1}$), the damage is lower than for commercial AMB
925 (109.8 ± 2.2 %) at the same concentration ($250 \mu\text{g.mL}^{-1}$).
926
927

928
929 When the AMB concentration was decrease to $62.5 \mu\text{g.mL}^{-1}$, no difference statistical
930 was observed for CGPLAP 1:1 + AMB and CGPLAP 1:10 + AMB, with a hemolysis
931 extended less than 5 %. CGPLAP 1:1 + AMB exert a stabilizing and protective effect
932 on the cells against hemolysis even at higher AMB concentration than the previously
933 reported systems.
934
935
936
937
938
939
940
941
942
943
944

3.8 Drug release

To investigate the potential CGPLAP nanoparticles as AMB drug delivery devices, an *in vitro* release experiment was carried out using PBS buffer with 0.25 % sodium lauryl sulfate as release medium (Fig 8).

The release profile shows a sustained drug delivery, with maximal release percentage of 42.6 ± 4.5 and 52.2 ± 3.9 % after 168 h, for CGPLAP 1:1 and CGPLAP 1:10, respectively. The highest release percentage was obtained for CGPLAP 1:10 nanoparticles, probably due to its lower DS (1.10), which promotes less interaction with AMB, releasing a higher amount of drug.

Similar release profile is found for chitosan and AMB complex, releasing approximately 21% in the first 24 h, followed by 44.5% release after 20 days of experiment [70].

3.9 *In vitro* antifungal test

Unloaded CGPLAP nanoparticles showed inhibition activity against all *C. albican* strains (Table 3). The minimum inhibitory concentration (MIC) values for CGPLAP 1:1 was similar to that of commercial amphotericin B. As far as we concern no previous report on polylactideantifungal activity has been reported MIC values of AMB-loaded CGPLAP 1:1 and 1 : 10 (Table 3) are half the figure observed for commercial AMB solution, a fact that may be due to a synergistic effect of copolymer which also exhibits antifungal activity. These results indicate that CGPLAP nanoparticles have great potential as nanocarrier delivery system.

4. Conclusions

Copolymers of cashew gum and L-Lactide were synthesized using two CG:PLA molar ratios. Nanoparticles were produced through equilibrium dialysis using DMSO as a solvent. The copolymer nanoparticles have similar particle size and zeta potential. The CGPLAP 1:10 shows better stability, but CGPLAP 1:1 exhibits a narrower particles size

1004
1005
1006 distribution. The potential use of CGPLAP nanoparticles as drug delivery device was
1007
1008 tested using AMB as a proof-of concept. A high efficiency of encapsulation was
1009
1010 obtained if compared with CGPLAP Pickering emulsion system previously reported,
1011
1012 however AMB was more aggregated in the self-assembling nanoparticle than in
1013
1014 Pickering emulsion, but less than in Fungizone®. Unloaded CGPLAP nanoparticles
1015
1016 showed inhibition activity against all *C. albican* strains. MIC values of AMB-loaded
1017
1018 CGPLA are smaller than that observed for commercial AMB solution, a fact that may
1019
1020 be due to a copolymer synergistic effect, indicating that the system has a good potential
1021
1022 as AMB nanocarrier delivery.

1022 **Acknowledgement**

1023
1024
1025 This study was partially supported by the Coordenação de Aperfeiçoamento de
1026
1027 Pessoal de Nível Superior (CAPES)-Finance code 001, by CNPq (Brazil),
1028
1029 INOMAT/INCT (Brazil) and FUNCAP (Brazil). The authors are grateful to the Central
1030
1031 Analítica-UFC/CT-INFRA/MCTI-SISANO/Pró-Equipamentos CAPES for the support
1032
1033 with SEM imaging and to CENAURENM for NMR analysis .
1034

1035 **References**

- 1036
1037 [1] I. Katouzian, S.M. Jafari, Nano-encapsulation as a promising approach for targeted
1038
1039 delivery and controlled release of vitamins, Trends Food Sci. Technol. 53 (2016) 34-48.
1040
1041 <https://doi.org/10.1016/j.tifs.2016.05.002>
- 1042 [2] Y. Wang, P. Li, T.T.D. Tran, J. Zhang, L. Kong, Manufacturing techniques and
1043
1044 surface engineering of polymer based nanoparticles for targeted drug delivery to cancer,
1045
1046 Nanomaterials. 6 (2016) 26. <https://doi.org/10.3390/nano6020026>
- 1047 [3] S. Gaurava, M. Ankita, S. Pradeep, Characterization and in vitro degradation studies
1048
1049 of synthesized polylactide (PLA), Res. J. Chem. Environ. 16 (2012), 14-21. ISSN: 0972-
1050
1051 0626
- 1052 [4] R.P. John, K.M.Nampoothiri, A.S. Nair, A Pandey, L (+)-lactic acid production
1053
1054 using *Lactobacillus casei* in solid-state fermentation, Biotechnol. Lett. 27 (2005), 1685-
1055
1056 1688. <https://doi.org/10.1007/s10529-005-2731-8>
- 1057 [5] Y. Guo, X. Wang, X. Shu, Z. Shen, R. Sun, Self-assembly and paclitaxel capacity of
1058
1059 cellulose-graft-poly (lactide) nanomicelles, J. Agr. Food. Chen. 60 (2012) 3900-
1060
1061 3908. <https://doi.org/10.1021/jf3001873>
1062

- 1063
1064
1065
1066
1067
1068
1069
1070
1071
1072
1073
1074
1075
1076
1077
1078
1079
1080
1081
1082
1083
1084
1085
1086
1087
1088
1089
1090
1091
1092
1093
1094
1095
1096
1097
1098
1099
1100
1101
1102
1103
1104
1105
1106
1107
1108
1109
1110
1111
1112
1113
1114
1115
1116
1117
1118
1119
1120
1121
- [6] H. Feng, C. Dong, Preparation, characterization and self-assembled properties of biodegradable chitosan-poly (L-lactide) hybrid amphiphiles, *Biomacromolecules* 7 (2006) 3069-3075. <https://doi.org/10.1021/bm060568l>
- [7] H. Yan, J. Wu, J. Zhang, J. He, J. Zhang, Hydrolytic degradation of cellulose-graft-poly(L-lactide) copolymers, *Polym. Degrad. Stabil.* 118 (2015) 130-136. <http://dx.doi.org/10.1016/j.polymdegradstab.2015.04.019>
- [8] W. Ge, Y. Guo, H. Zhong, X. Wang, R. Sun, Synthesis, characterization, and micellar behaviors of hydroxyethyl cellulose-graft-poly(lactide/ ϵ -caprolactone/*p*-dioxanone), *Cellulose* 22 (2015) 2365-2374. <https://doi.org/10.1007/s10570-015-0663-6>
- [9] R. Lipsa, N. Tudorachi, C. Vasile, A. Chiriac, A. Grigoras, Novel environmentally friendly copolymers carboxymethyl starch grafted poly(lactic acid), *J. Polym. Environ.* 21 (2013) 461-471. <https://doi.org/10.1007/s10924-012-0470-1>
- [10] H. Lu, H. He, B. Zhang, G. Liu, M. Li, Q. Nie, Facile synthesis of the amphiphilic chitosan-g-poly(lactic acid) derivatives and the study of their controlled drug release, *J. Appl. Polym. Sci.* 130 (2013), 908-915. <https://doi.org/10.1002/app.39205>
- [11] X. Tang, J. Huang, L. Xu, Y. Li, J. Song, Y. Ma, L. Yang, D. Yuan, H. Wu, Microwave-assisted rapid synthesis, characterization and application of poly (D,L-lactide)-graft-pullulan, *Carbohydr. Polym.* 107 (2014) 7-15. <http://dx.doi.org/doi:10.1016/j.carbpol.2014.02.038>
- [12] J. Cho, W. Park, K. Na, Self-organized nanogels from pullulan-g-poly(L lactide) synthesized by one-pot method: Physicochemical characterization and in vitro doxorubicin release, *J. Appl. Polym. Sci.* 113 (2009) 2209-2216. <https://doi.org/10.1002/app.30049>
- [13] S. Seo, C. Lee, Y. Jung, K. Na, Thermo-sensitivity and triggered drug release of polysaccharide nanogels derived from pullulan-g-poly (L-lactide) copolymers, *Carbohydr. Polym.* 87 (2012) 1105-1111. <https://doi.org/10.1016/j.carbpol.2011.08.061>
- [14] A.D. Martino, V. Sedlarik, Amphiphilic chitosan-grafted-functionalized polylactide acid based nanoparticles as a delivery system for doxorubicin and temozolomide co-therapy, *Int. J. Pharm.* 474 (2014) 134-145. <https://doi.org/10.1016/j.ijpharm.2014.08.014>
- [15] T.S Demina, T.A. Akopova, L.V. Vladimirov, A.N. Zelenetskii, E.A. Markivicheva, C. Grandgils, Polylactide-based microspheres prepared using solid-state copolymerized chitosan and D,L-lactide, *Mat. Sci. Eng. C*, 59 (2016) 333-338. <https://doi.org/10.1016/j.msec.2015.09.094>
- [16] Li, J., Kong, M., Cheng, X.J., Dang, Q.F., Zhou, X., Wei, Y.N. & Chen, X.G. (2012). Preparation of biocompatible chitosan grafted poly(lactic acid) nanoparticles. *Int. J. Biol. Macromol.* 51, 221-227. <http://dx.doi.org/10.1016/j.ijbiomac.2012.05.011>

- 1122
1123
1124
1125
1126
1127
1128
1129
1130
1131
1132
1133
1134
1135
1136
1137
1138
1139
1140
1141
1142
1143
1144
1145
1146
1147
1148
1149
1150
1151
1152
1153
1154
1155
1156
1157
1158
1159
1160
1161
1162
1163
1164
1165
1166
1167
1168
1169
1170
1171
1172
1173
1174
1175
1176
1177
1178
1179
1180
- [17] P.L.R. Cunha, R.C.M. de Paula, J.P.A. Feitosa, Polissacarídeos da biodiversidade brasileira: uma oportunidade de transformar conhecimento em valor econômico, Quím. Nova, 32 (2009) 649-660. <http://dx.doi.org/10.1590/S0100-40422009000300009>
- [18] R.C.M. de Paula, J.F. Rodrigues, Composition and rheological properties of cashew tree gum, the exudate polysaccharide from *Anacardium occidentale* L. Carbohyd. Polym. 26 (1995), 177-181. [https://doi.org/10.1016/0144-8617\(95\)00006-S](https://doi.org/10.1016/0144-8617(95)00006-S)
- [19] R.C.M. de Paula, F. Heatley, P.M. Budd, Characterization of *Anacardium occidentale* exudate polysaccharide, Polym. Int. 45 (1998) 27- 35. [https://doi.org/10.1002/\(SICI\)1097-0126\(199801\)45:1<27::AID-PI900>3.0.CO;2-9](https://doi.org/10.1002/(SICI)1097-0126(199801)45:1<27::AID-PI900>3.0.CO;2-9)
- [20] M.R. Guilherme, G.M. Campese, E. Radovanovic, A.F. Rubira, J.P.A. Feitosa, E.C. Muniz, Morphology and water affinity of superabsorbent hydrogels composed of methacrylated cashew gum and acrylamide with good mechanical properties, Polym. 46(2005a) 7867-7873. <https://doi.org/10.1016/j.polymer.2005.06.068>
- [21] M.R. Guilherme, A.V. Reis, A.H. Takahashi, A.F. Rubira, J.P.A. Feitosa, E.C. Muniz, Synthesis of a novel superabsorbent hydrogel by copolymerization of acrylamide and cashew gum modified with glycidyl methacrylate, Carbohyd. Polym. 61 (2005b) 464-471. <https://doi.org/10.1016/j.carbpol.2005.06.017>
- [22] D.A. da Silva, R.C.M. de Paula, J.P.A. Feitosa, Graftcopolymerization of acrylamide onto cashew gum, Eur. Polym. J. 43 (2007) 2620-2629. <https://doi.org/10.1016/j.eurpolymj.2007.03.041>
- [23] J.M. Klein, V.S. de Lima, J.M.C. da Feira, R.N. Brandalise, M.M.C. Forte, Chemical modification of cashew gum with acrylamide using an ultrasound-assisted method, J. Appl. Polym. Sci. 133 (2016) 43634-43645. <https://doi.org/10.1002/app.43634>
- [24] M.T. Ramesan, K. Surya, Synthesis, characterization and properties of cashew gum graft poly(acrylamide)/magnetite nanocomposites, J. Appl. Polym. Sci. 133 (2016) 43496-43504. <https://doi.org/10.1002/app.43496>
- [25] D.A. da Silva, J.P.A. Feitosa, H.C.B. Paula, R.C.M. de Paula, Synthesis and characterization of cashew gum/acrylic acid nanoparticles, Mat. Sci. Eng. C 29 (2009) 437-441. <https://doi.org/10.1016/j.msec.2008.08.029>
- [26] C.M.W. Abreu, H.C.B. Paula, V. Seabra, J.P.A. Feitosa, B. Sarmiento, R.C.M. de Paula, Synthesis and characterization of non-toxic and thermo-sensitive poly(N-isopropylacrylamide)-grafted cashew gum nanoparticles as a potential epirubicin delivery matrix, Carbohyd. Polym. 154 (2016) 77-85. <https://doi.org/10.1016/j.carbpol.2016.08.031>
- [27] J. Gomes-Estaca, T.A. Comunian, P. Montero, R. Ferro-Furtado, C.S. Favaro-Trindade, Encapsulation of an astaxanthin-containing lipid extract from shrimp waste by complex coacervation using a novel gelatin-cashew gum complex, Food Hydrocolloid. 61 (2016) 155-162. <https://doi.org/10.1016/j.foodhyd.2016.05.005>

- 1181
1182
1183
1184
1185
1186
1187
1188
1189
1190
1191
1192
1193
1194
1195
1196
1197
1198
1199
1200
1201
1202
1203
1204
1205
1206
1207
1208
1209
1210
1211
1212
1213
1214
1215
1216
1217
1218
1219
1220
1221
1222
1223
1224
1225
1226
1227
1228
1229
1230
1231
1232
1233
1234
1235
1236
1237
1238
1239
- [28] S.F.L. Dias, S.S. Nogueira, F.F. Dourado, M.A. Guimarães, N.A.O. Pitombeira, G.G. Gobbo, F.L. Primo, R.C.M. de Paula, J.P.A. Feitosa, A.C. Tedesco, L.C.C. Nunes, J.R.S.A. Leite, D.A. da Silva, Acetylated cashew gum-based nanoparticles for transdermal delivery of diclofenac diethyl amine, *Carbohydr. Polym.* 143 (2016) 254-261. <https://doi.org/10.1016/j.carbpol.2016.02.004>
- [29] N.A.O. Pitombeira, J.G. VerasNeto, D.A. Silva, J.P.A. Feitosa, H.C.B. Paula, R.C.M. Paula, Self-assembled nanoparticles of acetylated cashew gum: Characterization and evaluation as potential drug carrier, *Carbohydr. Polym.* 117 (2015) 610-615. <https://doi.org/10.1016/j.carbpol.2014.09.087>
- [30] M.R.L. Cardial, H.C.B. Paula, R.B.C. da Silva, J.F.S. Barros, A.R. Richter, F.M. Sombra, R.C.M. de Paula, Pickering emulsions stabilized with cashew gum nanoparticles as indomethacin carrier, *Int. J. Biol. Macromol.* 132 (2019) 534-540. <https://doi.org/10.1016/j.ijbiomac.2019.03.198>.
- [31] G.A. Magalhães Jr., C.M.W. Santos, D.A. Silva, J.S. Maciel, J.P.A. Feitosa, H.C.B. Paula, R.C.M. de Paula, Microspheres of chitosan/carboxymethyl cashew gum (CH/CMCG): Effect of chitosan molar mass and CMCG degree of substitution on the swelling and BSA release, *Carbohydr. Polym.* 77 (2009) 217-222. <https://doi.org/10.1016/j.carbpol.2008.12.037>
- [32] J.S. Maciel, H.C.B. Paula, M.A. Miranda, J.M. Sasaki, R.C.M. de Paula, Reacetylated chitosan/cashew gum gel: Preliminary study for potential utilization as drug release matrix, *J. Appl. Polym. Sci.* 99 (2006) 326-334. <https://doi.org/10.1002/app.22099>
- [33] B. Das, S. Dutta, A.K. Nayak, U. Nanda, Zinc alginate-carboxymethyl cashew gum microbeads for prolonged drug release: development and optimization, *Int. J. Biol. Macromol.* 70 (2014) 506-515. <https://doi.org/10.1016/j.ijbiomac.2014.07.030>
- [34] J.A. Rodrigues, A.R. de Araújo, N.A.O. Pitombeira, A. Plácido, M.P. de Almeida, L.C.M. Veras, C. Matos-Delerue, F.C.D.A. Lima, A.B. Neto, R.C.M. de Paula, J.P.A. Feitosa, P. Eaton, J.R.S. Leite, D.A. da Silva, Acetylated cashew gum-based nanoparticles for the incorporation of alkaloid epiisopiloturine, *Int. J. Biol. Macromol.* 128 (2019) 965-972. <https://doi.org/10.1016/j.ijbiomac.2019.01.206>
- [35] E.L.V. Silva, A.C.J. Oliveira, Y.B.G. Patriota, A.J. Ribeiro, F. Veiga, E.C.S.F. Hallwass, D.A. da Silva, M.F.R. Soares, A.G. Wanderley, J.L. Soares-Sobrinho, Solvent-free synthesis of acetylated cashew gum for oral delivery system of insulin, *Carbohydr. Polym.* 207 (2019) 601-608. <https://doi.org/10.1016/j.carbpol.2018.11.071>
- [36] A.R. Richter, J.P.A. Feitosa, H.C.B. Paula, F.M. Goycoolea, R.C.M. de Paula, Pickering emulsion stabilized by cashew gum- poly-L-lactide copolymer nanoparticles: Synthesis, characterization and amphotericin B encapsulation, *Colloid. Surfaces B* 164 (2018) 201–209. <https://doi.org/10.1016/j.colsurfb.2018.01.023>
- [37] N. Gold, H.A. Stout, J.F. Pagano, R. Donovan, Amphotericin A and B, antifungal antibiotics produced by a streptomycete I. *in vivo* studies, *Antibiotic Annual* 3 (1955-1956) 579-586

1240
1241
1242 [38] R.J. Hamill, Amphotericin B formulations: A comparative review of efficacy and
1243 toxicity, *Drugs* 73 (2013) 919. <https://doi.org/10.1007/s40265-013-0069-4>.
1244

1245 [39] B. Kruijff, R.A. Demel, Polyene antibiotic-sterol interactions in membranes
1246 of *Acholeplasma laidlawii* cells and lecithin liposomes. III. Molecular structure of the
1247 polyene antibiotic-cholesterol complexes, *Biochim. Biophys. Acta.* 339 (1974) 57-70.
1248 [https://doi.org/10.1016/0005-2736\(74\)90332-0](https://doi.org/10.1016/0005-2736(74)90332-0)
1249

1250 [40] T. Jabri, M. Imran, Shafiullah, K. Rao, I. Ali, M. Arfan, M.R. Shah, Fabrication of
1251 lecithin-gum tragacanth muco-adhesive hybrid nano-carrier system for in-vivo
1252 performance of Amphotericin B, *Carbohydr. Polym.* 194 (2018) 89–96.
1253 <https://doi.org/10.1016/j.carbpol.2018.04.013>
1254

1255 [41] R.G.J.V. Marcano, T.T. Tominaga, N.M. Khalil, L.S. Pedroso, R.M. Mainardes,
1256 Chitosan functionalized poly(ϵ -caprolactone) nanoparticles for amphotericin B delivery,
1257 *Carbohydr. Polym.* 202 (2018) 345–354. <https://doi.org/10.1016/j.carbpol.2018.08.142>
1258

1259 [42] M. R. Lima, H.C.B. Paula, F.O.M.S. Abreu, R.B.C. da Silva, F.M. Sombra, R.C.M.
1260 de Paula, Hydrophobization of cashew gum by acetylation mechanism and amphotericin
1261 B encapsulation, *Int. J. Biol. Macromol.* 108 (2018) 523-530.
1262 <https://doi.org/10.1016/j.ijbiomac.2017.12.047>
1263

1264 [43] V. Aparna, A.R. Melge, V.K. Rajan, R. Biswas, R. Jayakumar, C.G. Mohan,
1265 Carboxymethylated κ -carrageenan conjugated amphotericin B loaded gelatin
1266 nanoparticles for treating intracellular *Candida glabrata* infections. *Int. J. Biol.*
1267 *Macromol.* 110 (2018) 140–149. <https://doi.org/10.1016/j.ijbiomac.2017.11.126>
1268

1269 [44] Y. Wang, X.Ke, Z.X.Voo, S.S.L. Yap, C. Yang, S. Gao, S. Liu, S. Venkataraman,
1270 S.A.O.Obuobi, J.S.Khara, Y.Y. Yang, Biodegradable functional polycarbonate micelles
1271 for controlled release of amphotericin B, *Acta Biomater.* 46 (2016) 211-
1272 220. <https://doi.org/10.1016/j.actbio.2016.09.036>
1273

1274 [45] K. Gilani, E. Moazeni, T. Ramezanli, M. Amini, M.R. Fazeli, H. Jamalifar,
1275 Development of respirable nanomicelle carriers for delivery of amphotericin B by jet
1276 nebulization, *J. Pharm. Sci.* 100 (2011) 252–259. <https://doi.org/10.1002/jps.22274>
1277

1278 [46] K.K. Nishi, M. Antony, P.V. Mohanan, T.V. Anilkumar, P.M. Loiseau, A.
1279 Jayakrishnan, Amphotericin B-gum arabic conjugates: Synthesis, toxicity,
1280 bioavailability, and activities against *Leishmania* and fungi. *Pharm. Res.* 24 (2007)
1281 971–980. <https://doi.org/10.1007/s11095-006-9222-z>
1282

1283 [47] Z. Ishaq, N. Ahmed, M.N. Anwar, I. Haq, T. Rehman, N.M. Ahmad, A. Elaissari,
1284 Development and in vitro evaluation of cost effective amphotericin B polymeric
1285 emulsion, *J. Drug Deliv. Sci. Tec.* 46 (2018) 66–
1286 73. <https://doi.org/10.1016/j.jddst.2018.05.001>
1287

1288 [48] L. Sosa, B. Clares, H.L. Alvarado, N. Boza, O. Domenech, A.C. Calpena,
1289 Amphotericin B releasing topical nanoemulsion for the treatment of candidiasis and
1290 aspergillosis. *Nanomed-Nanotechnol.* 13 (2017) 2303–2312.
1291 <https://doi.org/10.1016/j.nano.2017.06.021>
1292
1293
1294
1295
1296
1297
1298

- 1299
1300
1301 [49] D.H. Donabedian, S.P. McCarthy, Acylation of pullulan by ring-opening of
1302 lactones, *Macromol.* 31 (1998) 1032-1039. <https://doi.org/10.1021/ma961741g>
1303
1304 [50] Y. Teramoto, Y. Nishio, Cellulose diacetate-graft-poly (lactic acid)s: Synthesis of
1305 wide-ranging compositions and their thermal and mechanical properties, *Polym.* 44
1306 (2003) 2701-2709. [https://doi.org/10.1016/S0032-3861\(03\)00190-3](https://doi.org/10.1016/S0032-3861(03)00190-3)
1307
1308 [51] Clinical and Laboratory Standards Institute. *Reference Method for Broth Dilution*
1309 *Antifungal Susceptibility Testing of Yeast*. Third Edition: Approved Standard M27-A3.
1310 CLSI: Wayne, PA, USA, 2008.
1311
1312 [52] L. Dai, D. Li, J. He, Degradation of grafted polymer and blend based on cellulose
1313 and poly (L-lactide), *J. Appl. Polym. Sci.* 130 (2013) 2257-2264.
1314 <https://doi.org/10.1002/app.39451>
1315
1316 [53] R. Liu, L. Dai, Z. Zhou, C. Si, Drug-loaded poly(L-lactide)/lignin stereocomplex
1317 film for enhancing stability and sustained release of trans-resveratrol, *Int. J. Biol.*
1318 *Macromol.* 119 (2018) 1129-1136. <https://doi.org/10.1016/j.ijbiomac.2018.08.040>
1319
1320 [54] A.H. Mijinyawa, G. Durga, A. Mishra, Isolation, characterization and microwave
1321 surface modification of *Colocasiaculenta*(L.) Schott mucilage by grafting
1322 polylactide, *Int. J. Biol. Macromol.* 119 (2018) 1090-
1323 1097. <https://doi.org/10.1016/j.ijbiomac.2018.08.045>
1324
1325 [55] C. Lee, C. Huang, Y. Lee, Preparation of amphiphilic poly (L-lactide)-graft
1326 chondroitin sulfate copolymer self-aggregates and its aggregation
1327 behavior, *Biomacromol.* 7 (2006) 1179-1186. <https://doi.org/10.1021/bm050995j>
1328
1329 [56] T.A. Dick, J. Couve, O. Gimello, A. Mas, J.J. Robin, Chemical modification and
1330 plasm-induced grafting of pyrolytic lignin. Evaluation of the reinforcing effect on
1331 lignin/poly(L-lactide), *Polym.* 118 (2017) 280-
1332 296. <http://dx.doi.org/10.1016/j.polymer.2017.04.036>
1333
1334 [57] P.L.R. Cunha, J.S. Maciel, M.R. Sierakowski, R.C.M. de Paula, J.P.A. Feitosa,
1335 Oxidation of cashew tree gum exudate polysaccharide with TEMPO reagent, *J. Brazil.*
1336 *Chem. Soc.* 18 (2007) 85-92. <http://dx.doi.org/10.1590/S0103-50532007000100009>
1337
1338 [58] H.C.B. Paula, F.J.S. Gomes, R.C.M. de Paula, Swelling studies of chitosan/cashew
1339 nut gum physical gels, *Carbohydr. Polym.* 48 (2002) 313-318.
1340 [https://doi.org/10.1016/S0144-8617\(01\)00264-8](https://doi.org/10.1016/S0144-8617(01)00264-8)
1341
1342 [59] D.A. Silva, R.C.M. de Paula, J.P.A. Feitosa, A.C.F. de Brito, J.S. Maciel, H.C.B.
1343 Paula, Carboxymethylation of cashew tree exudate polysaccharide, *Carbohydr. Polym.*
1344 58 (2004) 163-171. <https://doi.org/10.1016/j.carbpol.2004.06.034>
1345
1346 [60] E. Moura-Neto, J.S.M. Maciel, P.L.R. Cunha, R.C.M. de Paula, J.P.A. Feitosa,
1347 Preparation and characterization of a chemically sulfated cashew gum polysaccharide, *J.*
1348 *Brazil. Chem. Soc.* 22 (2011) 1953-1960. <http://dx.doi.org/10.1590/S0103-50532011001000017>
1349
1350
1351
1352
1353
1354
1355
1356
1357

- 1358
1359
1360
1361 [61] E.L. de Paula, F. Roig, A. Mas, J.P. Habas, V. Mano, F.V. Pereira, J.J. Robin,
1362 Effect of surface-grafted cellulose nanocrystals on the thermal and mechanical properties
1363 of PLLA based nanocomposites, *Eur.Polym. J.* 84 (2016). 173-187.
1364 <https://doi.org/10.1016/j.eurpolymj.2016.09.019>
- 1365
1366 [62] C. Lee, C. Huang, Y. Lee, Synthesis and characterization of amphiphilic poly (L-
1367 lactide)-graft-chondroitin sulfate copolymer and its application as drug carrier,*Biomol.*
1368 *Eng.* 24 (2007) 131-139. <https://doi.org/10.1016/j.bioeng.2006.05.010>
- 1369
1370 [63] C.R. Müller, S.A. Hass, V.L. Bassani, S.S. Guterres, H. Fessi, M.C.R. Peralba,
1371 A.R. Pohlmann, Degradação e estabilização do diclofenaco em
1372 nanocápsulaspoliméricas. *Quim. Nova*, 27 (2004) 555–560.
1373 <http://dx.doi.org/10.1590/S0100-40422004000400008>
- 1374
1375 [64] C.D. Rodrigues, K.N. Maissar, R.M. Mainardes, Determination of amphotericin B in
1376 PLA-PEG blend nanoparticles by HPLC-PDA, *Braz. J. Pharm. Sci.* 50 (2014) 859-868.
1377 <http://dx.doi.org/10.1590/S1984-82502014000400021>
- 1378
1379 [65] Z. Song, Y. Wen, P. Deng, F. Teng, F. Zhou, H. Xu, S. Feng, L. Zhu, R. Feng,
1380 Linolenic acid-modified methoxy poly (ethylene glycol)-oligochitosan conjugate
1381 micelles for encapsulation of amphotericin B, *Carbohydr. Polym.* 205 (2019) 571-
1382 580. <https://doi.org/10.1016/j.carbpol.2018.10.086>
- 1383
1384 [66] A.A. Ammar, A. Nasereddin, S. Ereqat, M. Dan-Goor, C.L. Jaffe, E. Zussman,
1385 Z. Abdeen, Amphotericin B-loaded nanoparticles for local treatment of cutaneous
1386 leishmaniasis, *Drug Deliv. Transl. Re.* 9 (2018) 76-84. [https://doi.org/10.1007/s13346-](https://doi.org/10.1007/s13346-018-00603-0)
1387 [018-00603-0](https://doi.org/10.1007/s13346-018-00603-0)
- 1388
1389 [67] Y. Kaneo, K. Taguchi, T. Tanaka, S. Yamamoto, Nanoparticles of hydrophobized
1390 cluster dextrin as biodegradable drug carriers: solubilization and encapsulation of
1391 amphotericin B, *J. Drug Deliv. Sci. Techn.* 24 (2014) 344-
1392 351. [https://doi.org/10.1016/S1773-2247\(14\)50072-X](https://doi.org/10.1016/S1773-2247(14)50072-X)
- 1393
1394 [68] J. Barwicz, S. Christian, I. Gruda, Effects of the aggregation state of amphotericin
1395 B on its toxicity to mice, *Antimicrob. Agents Ch.* 36 (1992) 2310–
1396 2315. <https://doi.org/10.1128/aac.36.10.2310>
- 1397
1398 [69] A.B. Mullen, K.C. Carter, A.J. Baillie, Comparison of the efficacies of various
1399 formulations of amphotericin B against murine visceral leishmaniasis, *Antimicrob.*
1400 *Agents Ch.* 41 (1997) 2089–2092. <https://doi.org/10.1128/AAC.41.10.2089>
- 1401
1402 [70] R.A. Krishnan, T. Pant, S. Sankaranarayan, J. Sternberg, R. Jain, P. Dandekar,
1403 Protective nature of low molecular weight chitosan in a chitosan–Amphotericin B
1404 nanocomplex – A physicochemical study, *Mat. Sci. Eng. C* 93 (2018) 472–
1405 482. <https://doi.org/10.1016/j.msec.2018.08.016>
- 1406
1407
1408
1409
1410
1411
1412
1413
1414
1415
1416

1417
1418
1419 **Legend list**
1420

1421 **Fig. 1.** ^1H NMR spectra for CGPLAP 1:10 and CGPLAP 1:1 in DMSO-d_6
1422

1423 **Fig. 2.** Stability of copolymers and particle size distribution over time (a), particle size
1424 distribution of CGPLAP 1:1 (b) and CGPLAP 1:10 (c) nanoparticles in phosphate
1425 buffer 7.4 at 37 °C.
1426
1427

1428 **Fig 3.** SEM micrographs of CGPLAP 1:1 (a) and CGPLAP 1:10 (b). AFM
1429 measurements of blank nanoparticles. AFM micrograph height images of CGPLAP
1430 1:1(c) and CGPLAP 1:10 (d) and AFM histograms graphics of CGPLAP 1:1(e) and
1431 CGPLAP 1:10(f) blank nanoparticles.
1432
1433

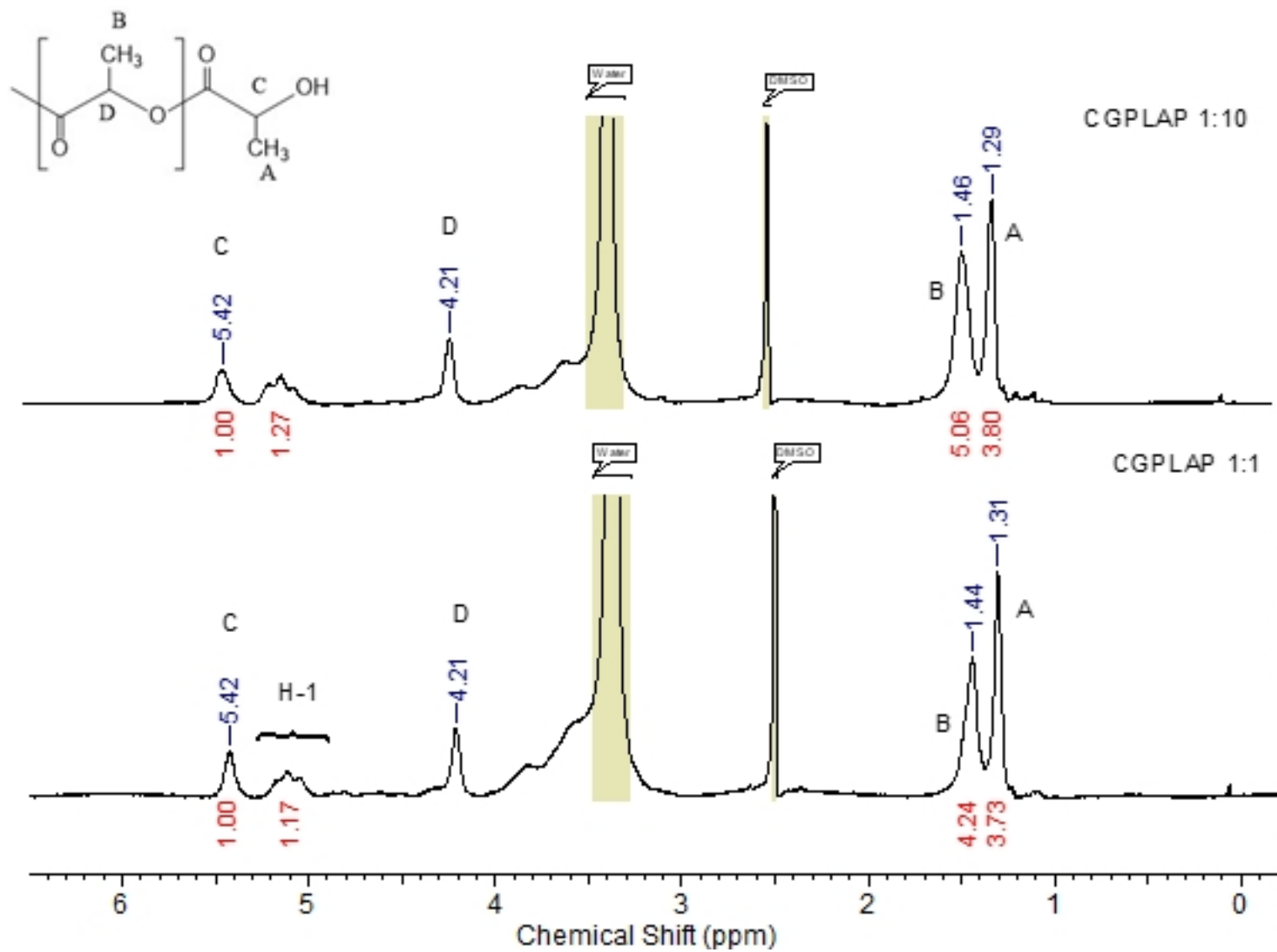
1434 **Fig. 4** AFM images of amplitude for (a) CGPLAP 1:1 and (b) CGPLAP 1:10 and phase
1435 images of (c) CGPLAP 1:1 and (d) CGPLAP 1:10 blank nanoparticles.
1436

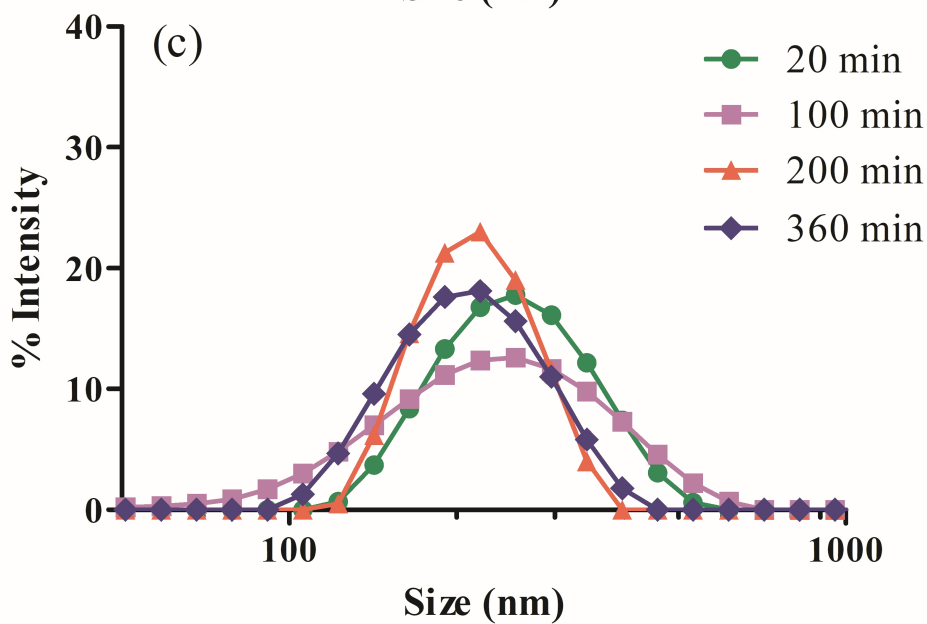
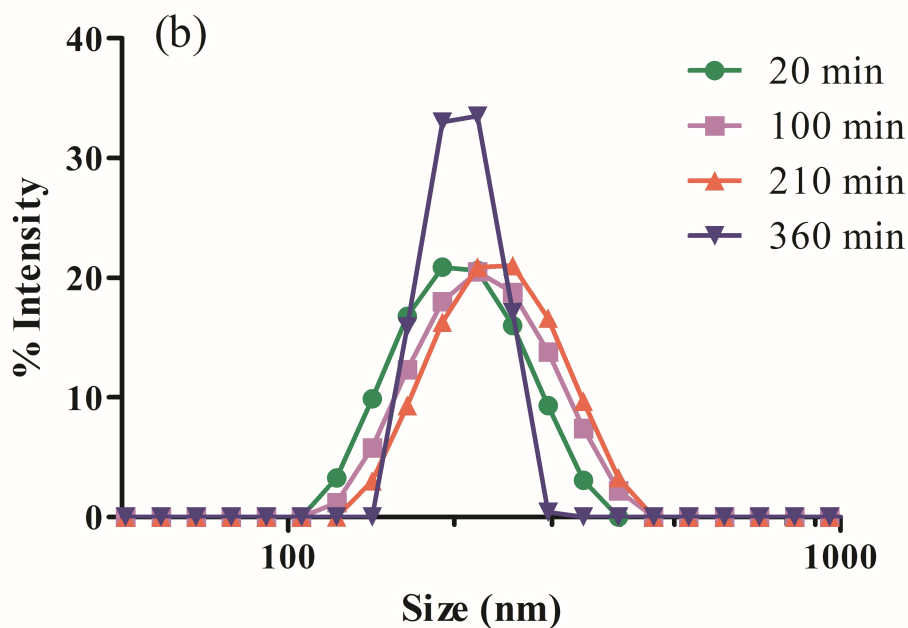
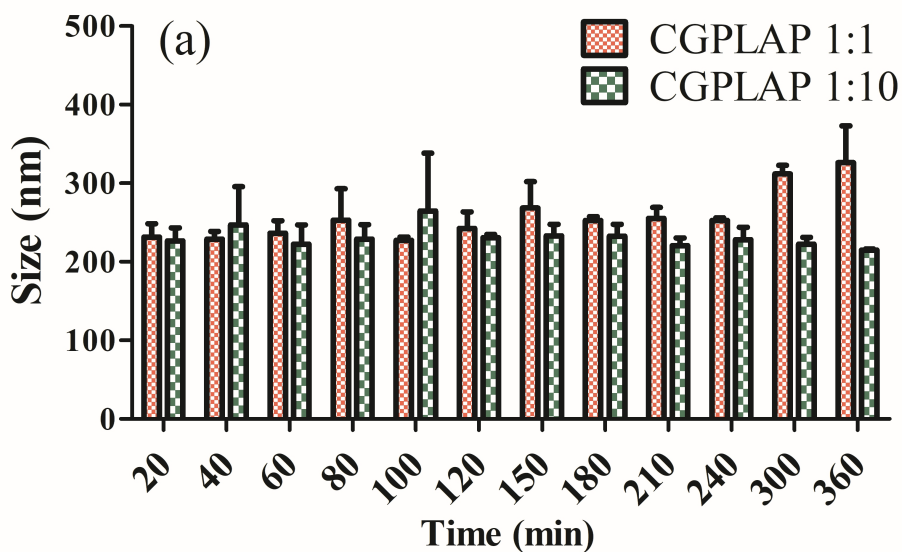
1437 **Fig. 5** UV-Vis spectra of AMB in DMSO and a commercial AMB aqueous
1438 solution (Sigma-Aldrich) (a) and AMB loaded CGPLAP nanoparticles aqueous solution
1439 (b).
1440
1441

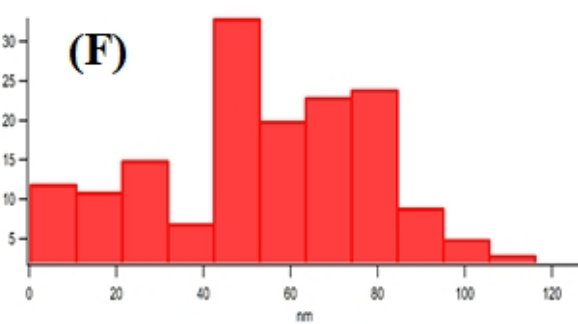
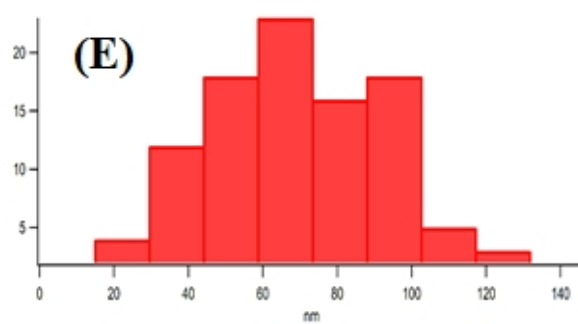
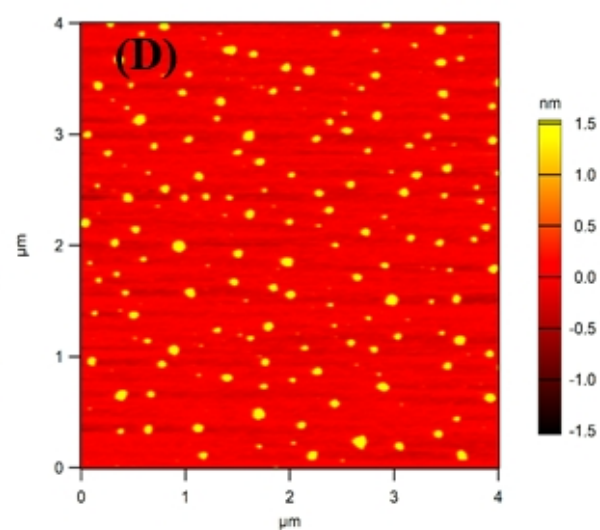
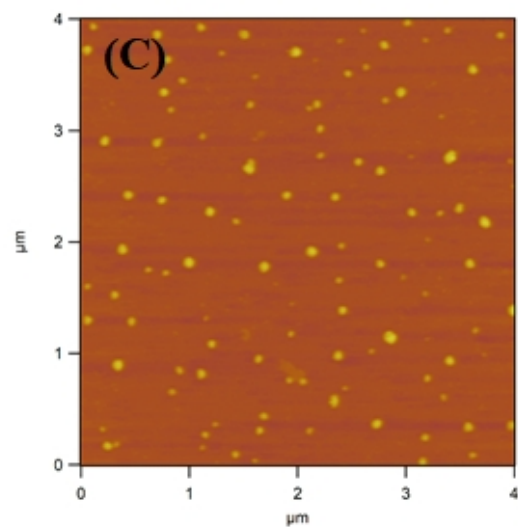
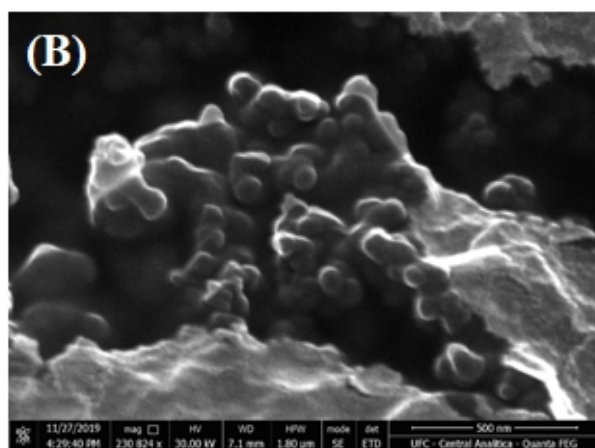
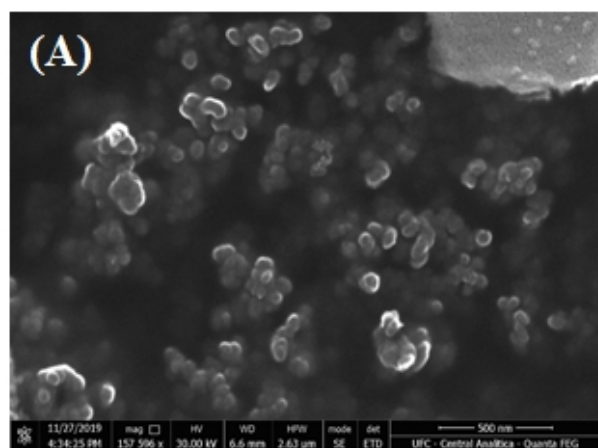
1442 **Fig 6.** Effect of AMB load on size, PDI and zeta potential for the CGPLAP
1443 nanoparticles.
1444

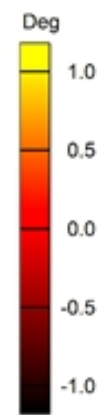
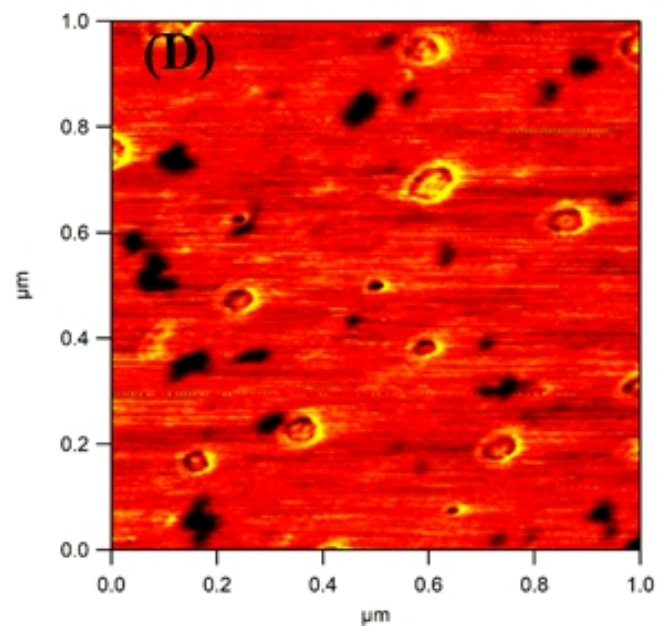
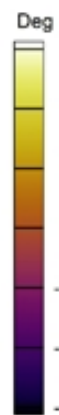
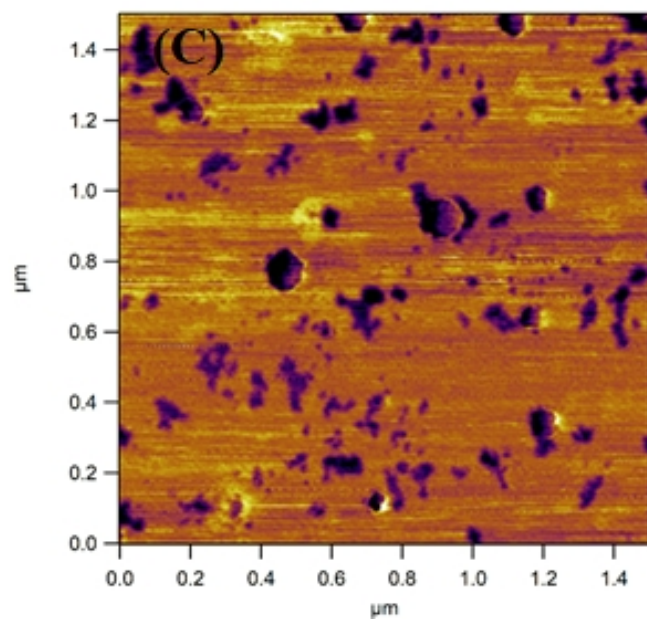
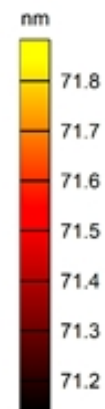
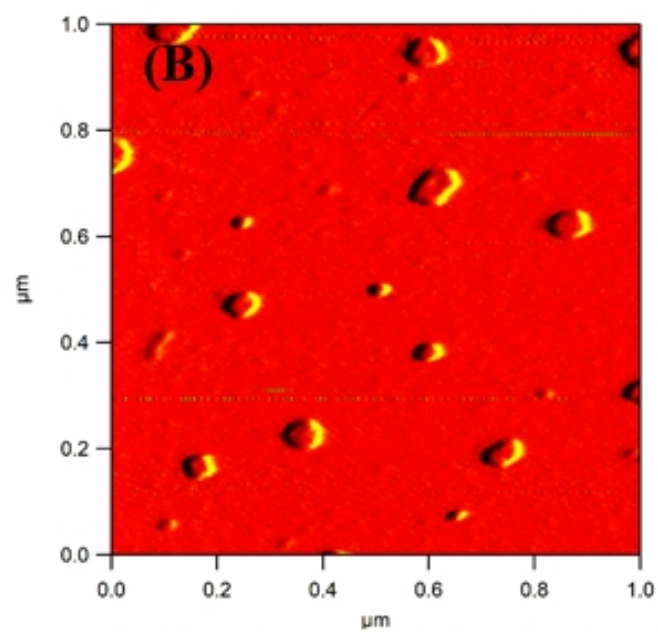
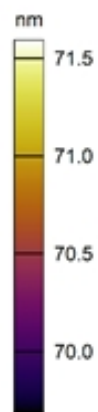
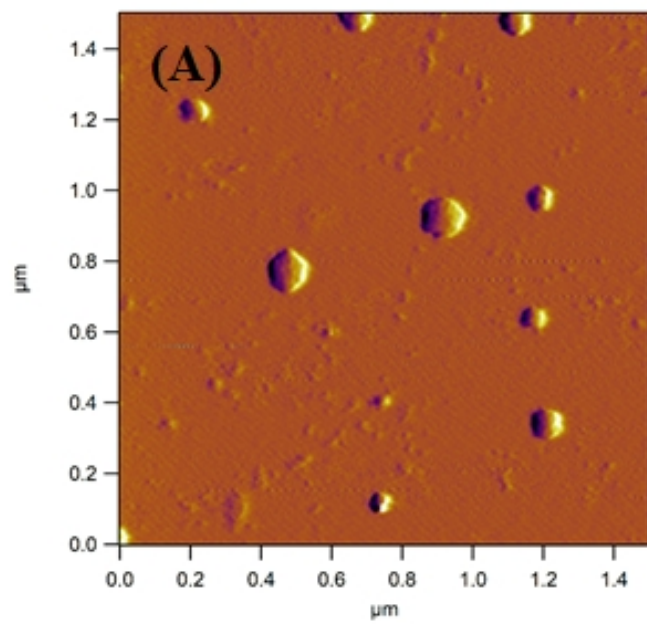
1445 **Fig. 7.** Hemolysis percentage as a function of concentration for CGPLAP 1:1 and
1446 CGPLAP 1:10 nanoparticles commercial AMB. Triton was used as a positive control.
1447

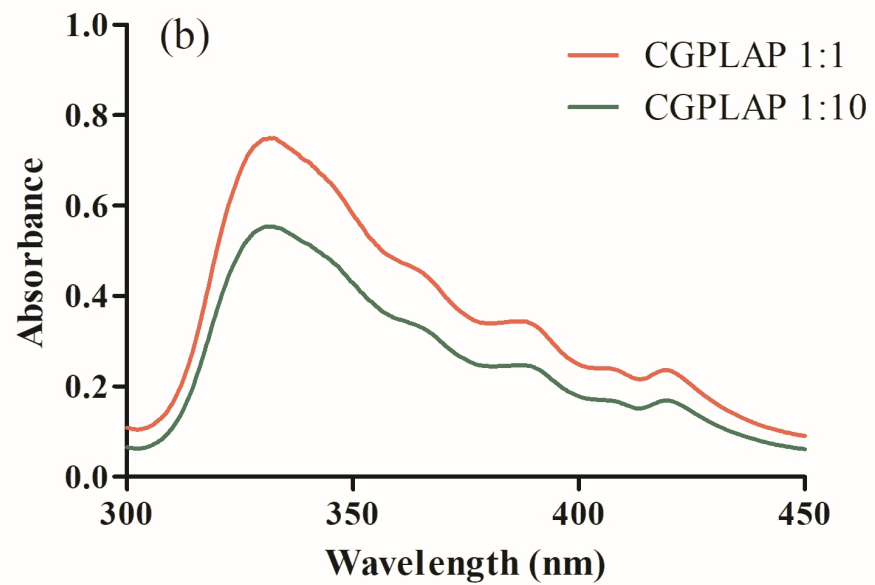
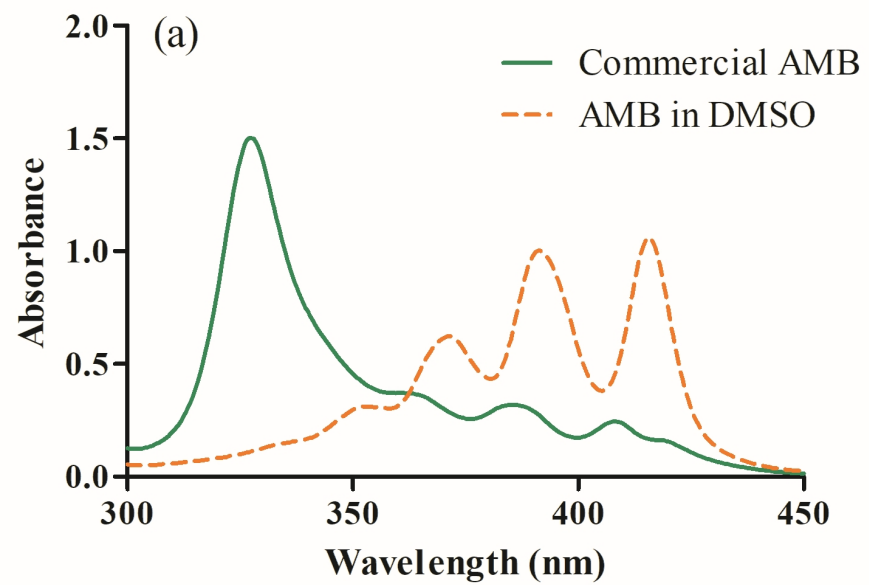
1448 **Fig 8.** *In vitro* AMB release profile for CGPLA nanoparticles nanocapsule in PBS buffer
1449 solution containing 0.25% sodium lauryl sulfate, at pH 7.4, and 37 °C
1450
1451
1452
1453
1454
1455
1456
1457
1458
1459
1460
1461
1462
1463
1464
1465
1466
1467
1468
1469
1470
1471
1472
1473
1474
1475

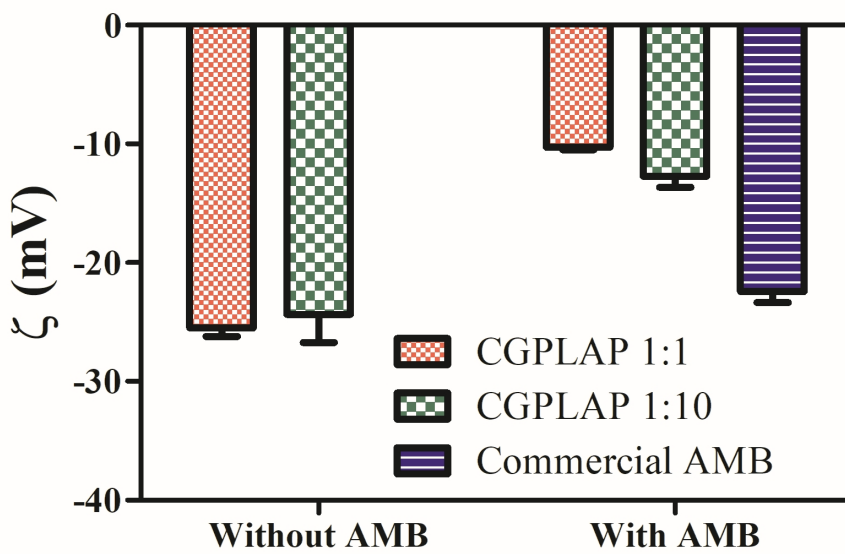
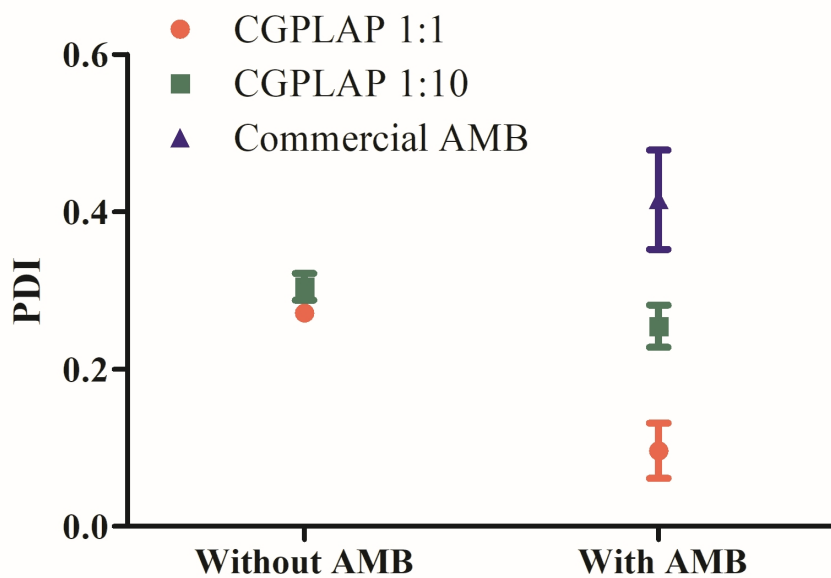
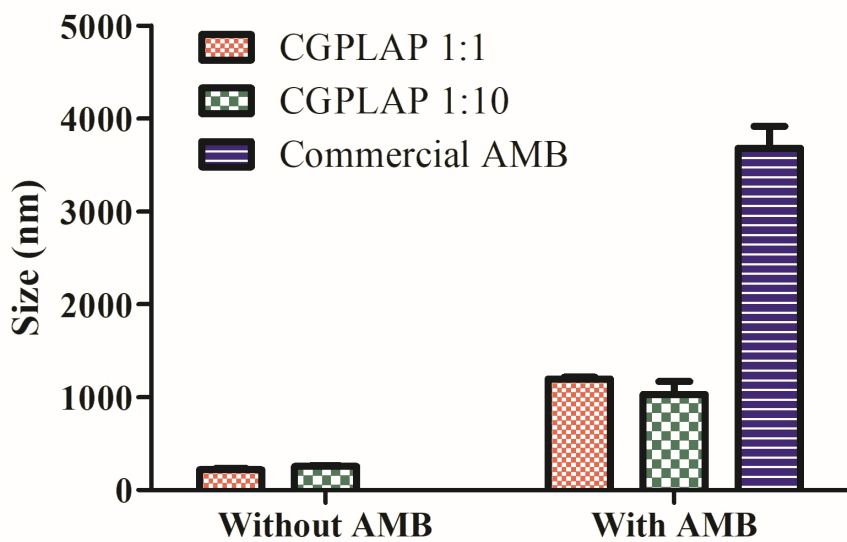


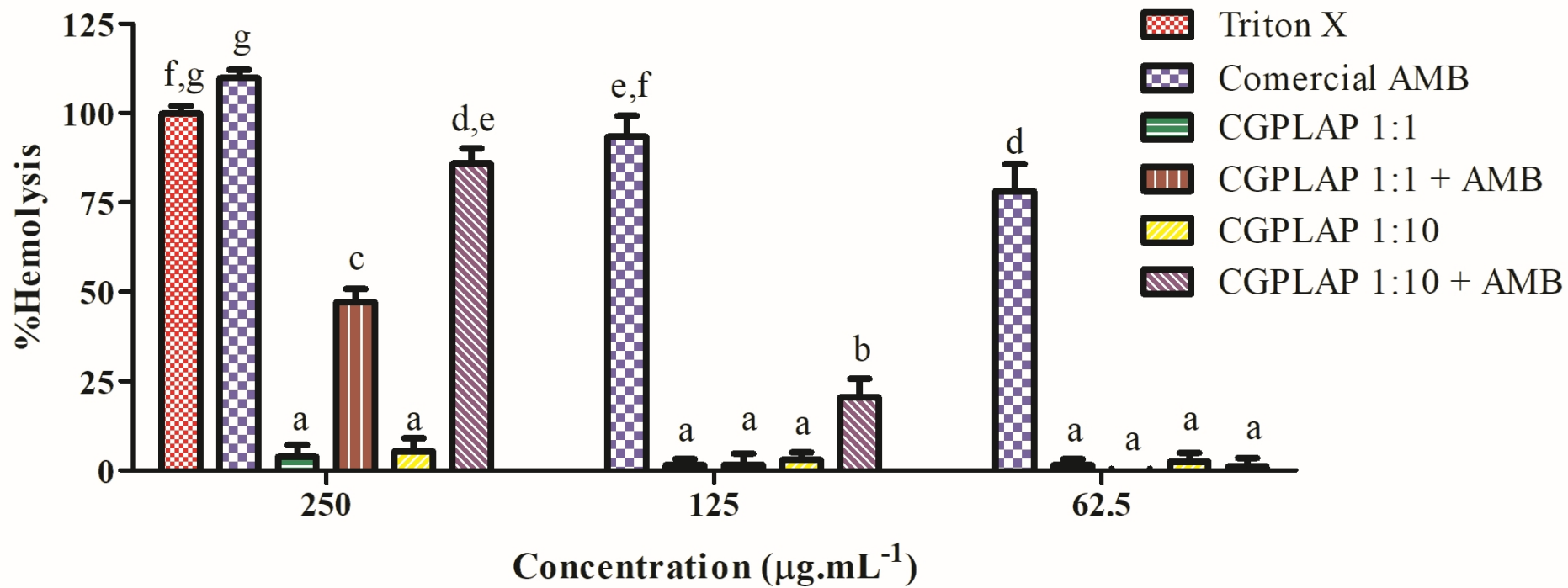


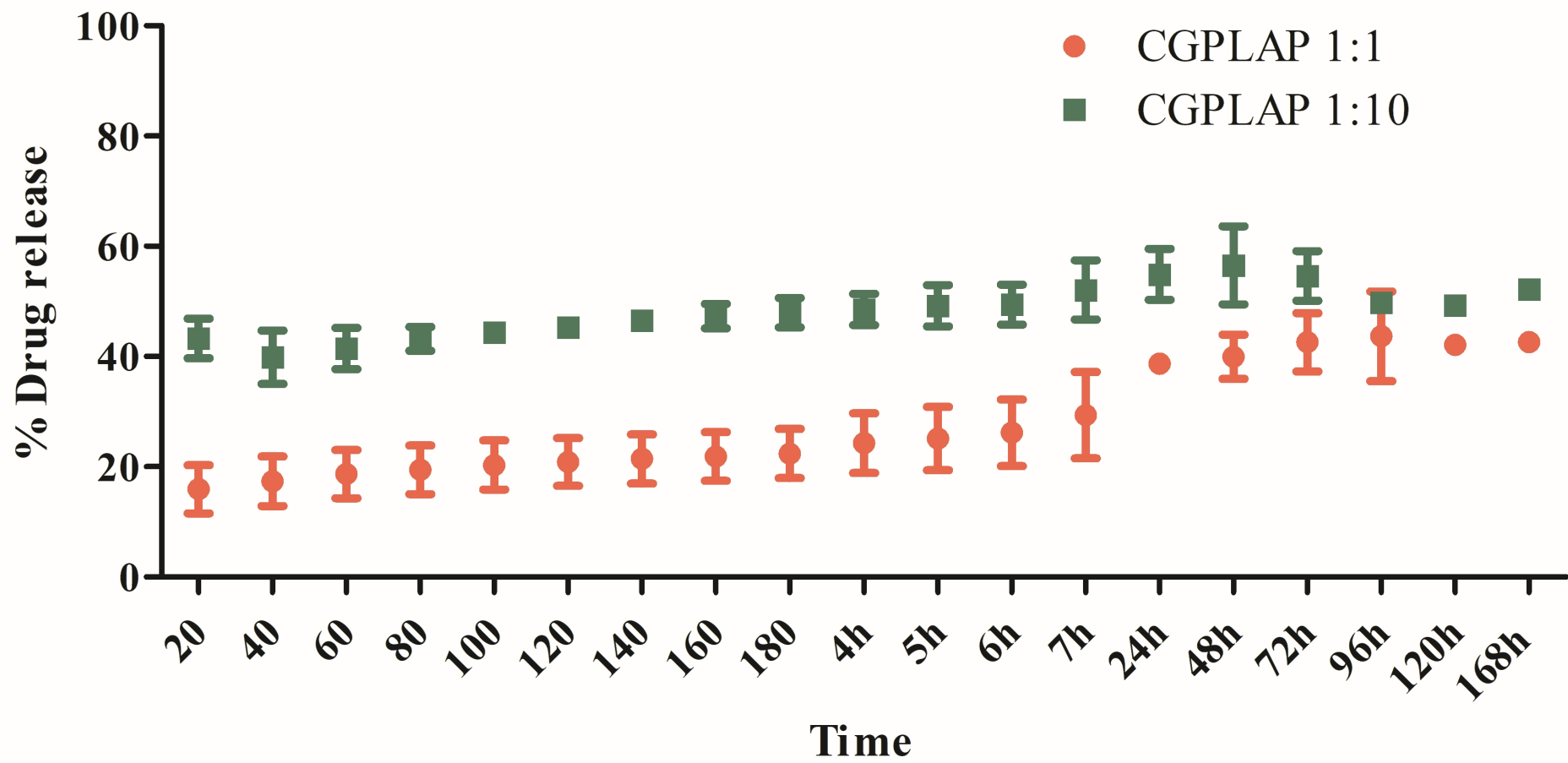


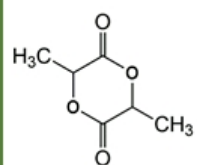




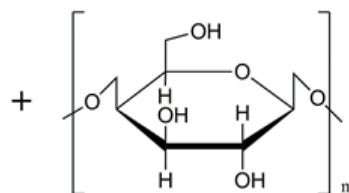






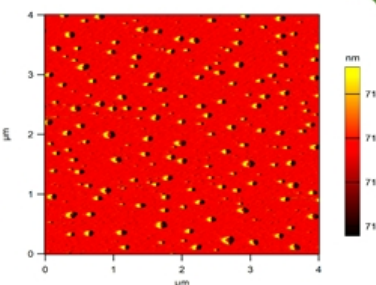
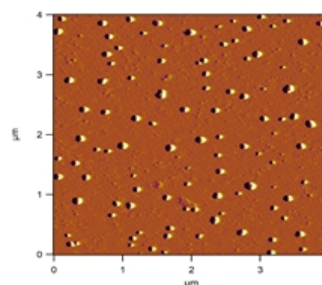
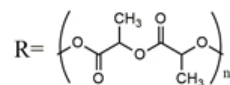
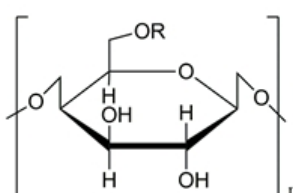


L-lactide



Cashew Gum

TEA
70 ~ 75 °C



self-assembled CGPLAP nanoparticles

	Size (nm)	PDI	Zeta potential
CGPLAP 1:1	230.4 ± 7.7	0.272 ± 0.002	-26.1 ± 1.9
CGPLAP 1:10	243.6 ± 10.7	0.307 ± 0.018	-24.3 ± 2.3

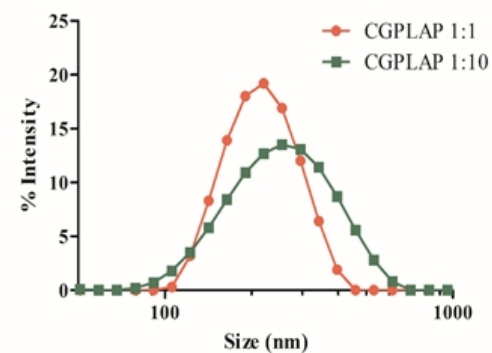


Table 1 - Amount of reagents and solvent used for the synthesis of CGPLAP copolymers

gum:L-lactide molar ratio ^a	DMSO (mL)	L-Lactide (g)	TEA (mL)
1:1	8.89	0.889	0.178
1:10	88.9	8.89	1.78

^aAmount of cashew gum was maintained at 1.0 g

Table 2- Yield and characteristics of copolymers obtained with different CG:PLA ratios.

Parameter	CG:PLA ratio	
	1:1	1:10
Reaction yield (%) ^a	66.5 ± 1.2	14.8 ± 0.7
Copolymer yield (%) ^b	98.2 ± 1.4	87.7 ± 5.4
Homopolymer yield (%) ^b	1.8 ± 1.4	12.3 ± 5.4
Grafting % ^c	18.7 ± 1.9	23.3 ± 7.7
MS	2.27	2.33
DS	1.06	1.00
DP	2.14	2.33

^a In relation to initial weight of CG+PLA; ^b in relation to unpurified copolymer; ^c mass of copolymer-mass of CG/mass of purified copolymer. MS, DS, and DP were calculated as described in equations 1 to 3.

Table 3. Minimum inhibitory concentration (MIC) against *Candida albicans* strains.

Samples	MIC ($\mu\text{g}\cdot\text{mL}^{-1}$)			
	<i>C. albicans</i>			
	ATCC 90028	LABMIC 0101	LABMIC 0102	LABMIC 0104
CGPLAP 1:1blank ^a	2	2	2	2
CGPLAP 1:10 blank ^a	1	1	1	1
AMB loaded CGPLAP 1:1	0.25	0.5	0.5	0.5
AMB loaded CGPLAP 1:1	0.5	0.5	0.5	0.5
AMB (Sigma)	1	1	1	1

^a Copolymer concentration

AUTHOR STATEMENT

Ana Rosa Richter- Investigation (synthesis, Physicochemical analysis, design methodology), analysis and discussion of results, writing original draft, visualization

Maria J. Carneiro- hemolysis experiments

Nayara A. de Sousa - hemolysis experiments

Vicente P. T. Pinto - hemolysis experiments

Rosimeyre S. Freire, R- *Nanoparticles Morphology analysis*

Jeanlex S. de Sousa *Nanoparticles Morphology analysis*

Josilayne de Fátima Souza Mendes antifungal activity

Raquel Oliveira dos Santos Fontenelle antifungal activity

Judith P. A. Feitosa - writing review analysis and discussion of results

Haroldo C. B. Paula- writing review analysis and discussion of results

Francisco M. Goycoolea- writing review analysis and discussion of results

Regina C. M. de Paula- funding acquisition, supervision, ideas, writing review, analysis and discussion of results